# USE OF MSE TECHNOLOGY TO STABILIZE HIGHWAY EMBANKMENTS AND SLOPES IN OKLAHOMA

## FINAL REPORT-FHWA-OK-11-04

ODOT SPR ITEM NUMBER 2214

by

Kianoosh Hatami

Assistant Professor

Gerald A. Miller

Professor

Danial Esmaili

PhD Student

School of Civil Engineering and Environmental Science

University of Oklahoma

Norman, OK

Research Division

Oklahoma Department of Transportation

200 NE 21$^{sh}$ Street

Oklahoma City, Oklahoma


March 2011

# TECHNICAL REPORT DOCUMENTATION PAGE

| | | |
|---|---|---|
| 1. REPORT NO.<br>FHWA - OK- 11- 04 | 2. GOVERNMENT ACCESSION NO. | 3. RECIPIENT=S CATALOG NO. |
| 4. TITLE AND SUBTITLE:<br>Use of MSE Technology to Stabilize Highway Embankments and Slopes in Oklahoma | | 5. REPORT DATE<br>March 2011<br>6. PERFORMING ORGANIZATION CODE |
| 7. AUTHOR(S) : Kianoosh Hatami, Gerald A. Miller and Danial Esmaili | | 8. PERFORMING ORGANIZATION REPORT |
| 9. PERFORMING ORGANIZATION NAME AND ADDRESS<br>School of Civil Engineering and Environmental Science, University of Oklahoma, Norman, OK | | 10. WORK UNIT NO.<br>11. CONTRACT OR GRANT NO.<br>ODOT SPR Item Number 2214 |
| 12. SPONSORING AGENCY NAME AND ADDRESS<br>Oklahoma Department of Transportation, Planning and Research Division, 200 N.E. 21st Street, Room 3A7, Oklahoma City, OK 73105 | | 13. TYPE OF REPORT AND PERIOD COVERED<br>Final Report<br>10/01/2009 – 09/30/2010<br>14. SPONSORING AGENCY CODE |
| 15. SUPPLEMENTARY NOTES | | |

16. ABSTRACT: Departments of transportation across the U.S. are faced with the persistent problem of landslides and slope failures along roads and highways. Repairs and maintenance work associated with these failures cost these agencies millions of dollars annually. Over the past few decades, Mechanically Stabilized Earth (MSE) technology has been successfully used as a cost-effective solution for the construction and repair of slopes and retaining structures in transportation applications. Significant cost-savings in the re-construction and repair of highway slopes and embankments could be achieved by using locally available soils and reinforcing them with geosynthetics. However, locally available soils in many locations are of marginal quality and their shear strength and interaction with the geosynthetic reinforcement can be significantly dependent on their moisture content. As a result, the influence of soil moisture content and suction on the soil-reinforcement interaction needs to be properly accounted for in the design of reinforced soil slopes and embankments. Provisions related to the influence of soil suction on the shear strength of soil-reinforcement interfaces are currently lacking in the existing design guidelines for these structures. In this study, a moisture reduction factor was developed for the pullout resistance of a geotextile reinforcement material in an Oklahoma soil (termed here as Chickasha soil) that could be used for the design of reinforced soil structures with marginal soils.

| | | | |
|---|---|---|---|
| 17. KEY WORDS: Mechanically stabilized earth, Slope stability, Marginal soil, Geosynthetics, Moisture reduction factor | 18. DISTRIBUTION STATEMENT<br>No restrictions. This publication is available from the planning and research Div., Oklahoma DOT. | | |
| 19. SECURITY CLASSIF. (OF THIS REPORT)<br>Unclassified | 20. SECURITY CLASSIF. (OF THIS PAGE)<br>Unclassified | 21. NO. OF PAGES<br>77 | 22. PRICE<br>N/A |

# * (MODERN METRIC) CONVERSION FACTORS

| APPROXIMATE CONVERSIONS TO SI UNITS | | | | |
|---|---|---|---|---|
| **SYMBOL** | **WHEN YOU KNOW** | **MULTIPLY BY** | **TO FIND** | **SYMBOL** |
| **LENGTH** | | | | |
| **in** | inches | 25.4 | millimeters | mm |
| **ft** | feet | 0.305 | meters | m |
| **yd** | yards | 0.914 | meters | m |
| **mi** | miles | 1.61 | kilometers | km |
| **AREA** | | | | |
| **$in^2$** | square inches | 645.2 | square millimeters | $mm^2$ |
| **$ft^2$** | square feet | 0.093 | square meters | $m^2$ |
| **$yd^2$** | square yard | 0.836 | square meters | $m^2$ |
| **ac** | acres | 0.405 | hectares | ha |
| **$mi^2$** | square miles | 2.59 | square kilometers | $km^2$ |
| **VOLUME** | | | | |
| **fl oz** | fluid ounces | 29.57 | milliliters | mL |
| **gal** | gallons | 3.785 | liters | L |
| **$ft^3$** | cubic feet | 0.028 | cubic meters | $m^3$ |
| **$yd^3$** | cubic yards | 0.765 | cubic meters | $m^3$ |
| NOTE: volumes greater than 1000 L shall be shown in $m^3$ | | | | |
| **MASS** | | | | |
| **oz** | ounces | 28.35 | grams | g |
| **lb** | pounds | 0.454 | kilograms | kg |
| **T** | short tons (2000 lb) | 0.907 | megagrams (or "metric ton") | Mg (or "t") |
| **TEMPERATURE (exact degrees)** | | | | |
| **$^oF$** | Fahrenheit | 5 (F-32)/9<br>or (F-32)/1.8 | Celsius | $^oC$ |
| **ILLUMINATION** | | | | |
| **fc** | foot-candles | 10.76 | lux | lx |
| **fl** | foot-Lamberts | 3.426 | $candela/m^2$ | $cd/m^2$ |
| **FORCE and PRESSURE or STRESS** | | | | |
| **lbf** | poundforce | 4.45 | newtons | N |
| **$lbf/in^2$** | poundforce per square inch | 6.89 | kilopascals | kPa |

| APPROXIMATE CONVERSIONS FROM SI UNITS | | | | |
|---|---|---|---|---|
| **SYMBOL** | **WHEN YOU KNOW** | **MULTIPLY BY** | **TO FIND** | **SYMBOL** |
| **LENGTH** | | | | |
| **mm** | millimeters | 0.039 | inches | in |
| **m** | meters | 3.28 | feet | ft |
| **m** | meters | 1.09 | yards | yd |
| **km** | kilometers | 0.621 | miles | mi |
| **AREA** | | | | |
| **$mm^2$** | square millimeters | 0.0016 | square inches | $in^2$ |
| **$m^2$** | square meters | 10.764 | square feet | $ft^2$ |
| **$m^2$** | square meters | 1.195 | square yards | $yd^2$ |
| **ha** | hectares | 2.47 | acres | ac |
| **$km^2$** | square kilometers | 0.386 | square miles | $mi^2$ |
| **VOLUME** | | | | |
| **mL** | milliliters | 0.034 | fluid ounces | fl oz |
| **L** | liters | 0.264 | gallons | gal |
| **$m^3$** | cubic meters | 35.314 | cubic feet | $ft^3$ |
| **$m^3$** | cubic meters | 1.307 | cubic yards | $yd^3$ |
| **MASS** | | | | |
| **g** | grams | 0.035 | ounces | oz |
| **kg** | kilograms | 2.202 | pounds | lb |
| **Mg (or "t")** | megagrams (or "metric ton") | 1.103 | short tons (2000 lb) | T |
| TEMPERATURE (exact degrees) | | | | |
| **°C** | Celsius | 1.8C+32 | Fahrenheit | °F |
| **ILLUMINATION** | | | | |
| **lx** | lux | 0.0929 | foot-candles | fc |
| **$cd/m^2$** | candela/$m^2$ | 0.2919 | foot-Lamberts | fl |
| **FORCE and PRESSURE or STRESS** | | | | |
| **N** | newtons | 0.225 | poundforce | lbf |
| **kPa** | kilopascals | 0.145 | poundforce per square inch | $lbf/in^2$ |

*SI is the symbol for the International System of Units. Appropriate rounding should be made to comply with Section 4 of ASTM E380.
(Revised March 2003)

The contents of this report reflect the views of the author(s) who is responsible for the facts and accuracy of the data presented herein. The contents do not necessarily reflect the views of the Oklahoma Department of transportation or the federal Highway Administration. This report does not constitute a standard, specification, or regulation. While trade names may be used in this report, it is not intended as an endorsement of any machine, contractor, process, or product.

## TABLE OF CONTENT

## LIST OF FIGURES

# LIST OF TABLES

# 1. INTRODUCTION

Oklahoma Department of Transportation (ODOT) and other departments of transportation across the U.S. are faced with a persistent problem of landslides and slope failures along the highways. Repairs and maintenance work due to these failures are extremely costly (i.e. in millions of dollars annually nationwide). In Oklahoma, many of these failures occur in the eastern and central parts of the state due to higher topography and poor soil type (Hatami et al. 2010a,b, 2011). A recent example of these failures is the landslide on the US Route 62 in Chickasha, Oklahoma. (**Figure 1**)

(a) (b)

Figure 1. A failed slope of a highway embankment in Chickasha, OK

For proper construction or repair of highway slopes and embankments an ideal solution would be to work with large quantities of coarse-grained, free-draining soils to stabilize the structures as recommended by design guidelines and specifications for Mechanically Stabilized Earth (MSE) structures in North America (e.g. Elias et al. 2001, Berg et al. 2009). However, coarse-grained soils are not commonly available in Oklahoma and many other parts of the U.S. Consequently, the costs of the fill material and its transportation can be prohibitive depending on the location of the high-quality soil.

One possible solution in such cases would be to use locally available soils as construction materials because they would require significantly less material transportation, fuel consumption and generated pollution compared to using high-quality offsite soils. It has been estimated the fuel costs constitute about 20% of the total costs for transportation of high-quality soil (Ou et al.

1982). On the other hand, commonly available soils in Oklahoma for the construction of reinforced slopes are of marginal quality (e.g., soils with more than 15% fines). Geosynthetic reinforcement can be used to stabilize marginal soils. Using the Mechanically Stabilized Earth technology (MSE) could help reduce the cost of fill material by up to 60% (Keller 1995). However, in order to reinforce earthen structures involving marginal soils, it is important to obtain a satisfactory soil-reinforcement interface performance. The performance of marginal soils and their interface with geosynthetic reinforcement can be complex under construction or service loading conditions and may include strain softening behavior, excessive deformation and loss of strength as a result of wetting.

An important consideration in the design of reinforced soil structures constructed with marginal soils is the possibility of reduction in interface pullout resistance due to the increase in the soil moisture content (wetting), loss of suction and possible development of excess pore water pressure. This can result in excessive deformations and even failure of the reinforced soil structure. As a result, the design procedures need to take into account the influence of soil moisture content on soil strength, the strength of soil-geosynthetic interface and the resulting factor of safety against failure. Such design provisions are currently not available for reinforced soil structures constructed with marginal soils. Typically, construction materials for reinforced soil structures are tested at moisture content values near optimum (i.e. Optimum Moisture Content - OMC). However, in actual construction, several factors could make the fill moisture content deviate from the design value. Examples include precipitation during construction, groundwater infiltration and development of excess pore water pressure due to compaction. These factors, in addition to seasonal variations of soil moisture content, can significantly reduce the strength of the soil-reinforcement interface and lead to excessive deformations or failure. A primary objective of this study is to develop a moisture reduction factor (MRF) for the pullout resistance of soil-geotextile interface for the design of reinforced soil structures with marginal soils.

It should be noted that this study is not intended to substitute the need for an adequate and properly located and constructed drainage system in reinforced soil structures and slopes. In addition, quality control and quality assurance in both design and construction of these structures are obviously required. In order for reinforced soil structures with marginal soils to be safe and provide satisfactory performance, a number of crucial factors need to be included in their design and construction including proper drainage systems, quality control during compaction (i.e. placement moisture content and density), small spacing between reinforcement

layers and relatively low construction speed to avert the consequences of loss of suction in the backfill.

## 2. THEORY

### 2.1. REINFORCEMENT PULLOUT CAPACITY IN MSE STRUCTURES

For internal stability, the pullout resistance per unit width ($P_r$) of the reinforcement is determined using **Equation 1** and it is defined as the ultimate tensile load required to generate outward sliding of the reinforcement through the reinforced soil mass (Elias et al. 2001, Berg et al. 2009):

$$P_r = F^* \, \alpha \, \sigma_v' \, L_e \, C \tag{1}$$

Where:

$L_e$: Embedment or adherence length in the resisting zone behind the failure surface

$C$: Reinforcement effective unit perimeter; e.g., C = 2 for strips, grids, and sheets

$L_e \, C$: Total surface area per unit weight of reinforcement in the resistive zone behind the failure surface

$F^* = \tan \delta_{peak}$ : Pullout resistance factor

$\delta_{peak}$: Equivalent peak friction angle of the soil-geosynthetic interface

$\alpha$: A scale effect correction factor to account for a nonlinear stress reduction over the embedded length of highly extensible reinforcements

$\sigma_v'$: Effective vertical stress at the soil-reinforcement interface

Pullout tests are typically used to obtain the parameters $\alpha$ and $F^*$ for different reinforcement materials. The correction factor α depends on the extensibility and the length of the reinforcement. For extensible sheets (i.e., geotextiles), the recommended value of $\alpha$ is 0.6 (Berg et al. 2009). The parameter $F^*$ (especially in reinforcement types such as geogrids and welded

wire mesh) includes both passive and frictional resistance components (e.g., Palmeira 2004, Abu-Farsakh et al. 2005, Berg et al. 2009).

Routine pullout tests are useful for determining short-term pullout capacity or reinforcement materials. However, they do not account for soil or reinforcement creep deformations. Tests are typically performed on samples with a minimum embedded length of 600 mm (24") as recommended in related guidelines (e.g. ASTM D6706). The pullout resistance ($P_r$) is taken as the peak pullout resistance value from the pullout tests.

## 2.2. EXTENDED MOHR-COULOMB FAILURE ENVELOPE

The shear strength of an unsaturated soil depends on two stress variables: net normal stress ($\sigma_n - u_a$) and soil matric suction ($u_a - u_w$) (Fredlund et al. 1978). Net normal stress is the difference between the total stress and pore air pressure, and the matric suction is the difference between the pore air and the pore water pressures. This theory is also valid for dry and saturated soil conditions. Miller and Hamid (2005) proposed the following equation to determine the shear strength of unsaturated soil-structure interfaces:

$$\tau_s = C_a' + (\sigma_n - u_a)\tan\delta' + (u_a - u_w)\tan\delta^b \quad (2)$$

Where:

$C_a'$: Adhesion intercept

$\sigma_n$: Normal stress on the interface

$u_a$: Pore air pressure

$\delta'$: The angle of friction between soil and reinforcement with respect to $(\sigma_n - u_a)$

$u_w$: Pore water pressure

$\delta^b$: The angle of friction between soil and reinforcement with respect to suction $(u_a - u_w)$

In the case of an unsaturated soil, Mohr circles representing failure conditions correspond to a 3D failure envelope, where the shear stress ($\tau$) is the ordinate and the two stress variables are the abscissas ($\sigma_n - u_a$) and ($u_a - u_w$). The locations of the Mohr circles in the third dimension

are functions of matric suction $(u_a - u_w)$. The planar surface formed by these two stress variables is called the extended Mohr-Coulomb failure envelope.

## 3. MATERIAL PROPERTIES AND SUCTION SENSORS

### 3.1. SOIL PROPERTIES

The soil used in the pullout tests for this study is a lean clay found on US Route 62 in Chickasha, OK (**Figure 2**). In this report, the soil is referred to as the Chickasha soil. Physical and mechanical soil property tests were carried out on the soil samples in general accordance with ASTM D1140 to determine the fines content and ASTM D422 for sieve analysis and hydrometer test. The results are given in **Figure 3** and **Table 1**. According to the Unified Soil Classification System (USCS) and AASHTO, the soil is classified as CL and A-6, respectively.

Figure 2. Excavation pit where soil samples were taken from the failed slope in Chickasha, OK

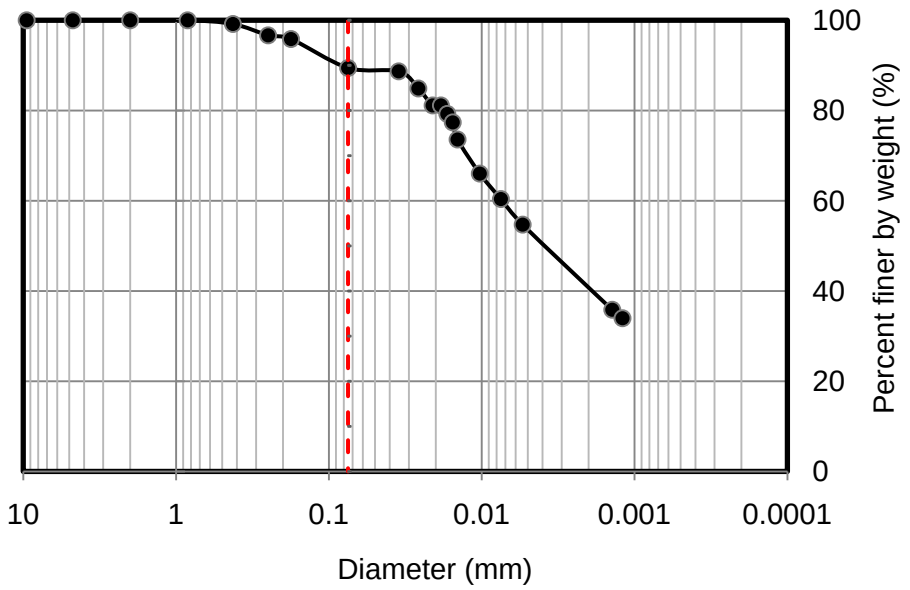


Figure 3. Gradation curve (sieve analysis) of Chickasha soil (The vertical broken line shows the location of #200 sieve)

Table 1. Summary of Chickasha soil properties

| Property (Lean clay) | Value |
|---|---|
| *Liquid Limit (%)* | 38 |
| *Plastic Limit (%)* | 20 |
| *Plasticity Index (%)* | 18 |
| *Specific Gravity* | 2.75 |
| *Gravel (%)* | 0 |
| *Sand (%)* | 10.6 |
| *Silt (%)* | 49.4 |
| *Clay (%)* | 40 |
| *Maximum Dry Unit Weight, kN/m$^3$ (pcf)* | 17.3 (111) |
| *Optimum Moisture Content (%)* | 18 |

Four compaction tests (one standard, two Harvard miniature, and one modified proctor test) were carried out on the Chickasha soil to determine the values of the soil maximum dry unit weight and optimum moisture content (**Figure 4**) more accurately. **Figure 4** also shows a series of theoretical curves of the soil dry unit weight versus moisture content for different degrees of saturation. These curves show different values of degree of saturation at maximum dry unit weight that were obtained from **Equation 3**:

$$\gamma_d = \left(\frac{G_s}{1+\frac{\omega G_s}{S}}\right)\gamma_w \quad (3)$$

Where:

$G_s$: Specific gravity

$\omega$: Moisture content

$S$: Degree of saturation

$\gamma_w$: Water unit weight

$\gamma_d$: Soil dry unit weight

The curves corresponding to S = 1, 0.9 and 0.8 are shown as the zero air void line (ZAVL - representing the minimum void ratio attainable at a given moisture content), 10% AVL and 20% AVL, respectively (Budhu, 2000). The air void lines in **Figure 4** were determined from **Equation 3**. To plot the ZAVL, the soil saturation was set to unity (S = 1). Then, having specific gravity for Chickasha soil from **Table 1** ($G_s$ = 2.75) and water unit weight ($\gamma_w$= 10 kN/m$^3$), the dry unit weight ($\gamma_d$) was calculated at different moisture content (ω) values. This procedure was repeated to obtain the 5%, 10%, 15% and 20% air void lines. **Figure 4** shows that the maximum dry unit weight was attained at S = 0.9 and also, the test results are reliable because the wetting points are placed below the ZAVL. Based on the results of all compaction tests, the best values for the maximum dry unit weight and optimum moisture content were chosen as $\gamma_{dmax}$ = 17.3 kN/m$^3$ (111 lb/ft$^3$) and OMC = 18%, respectively.

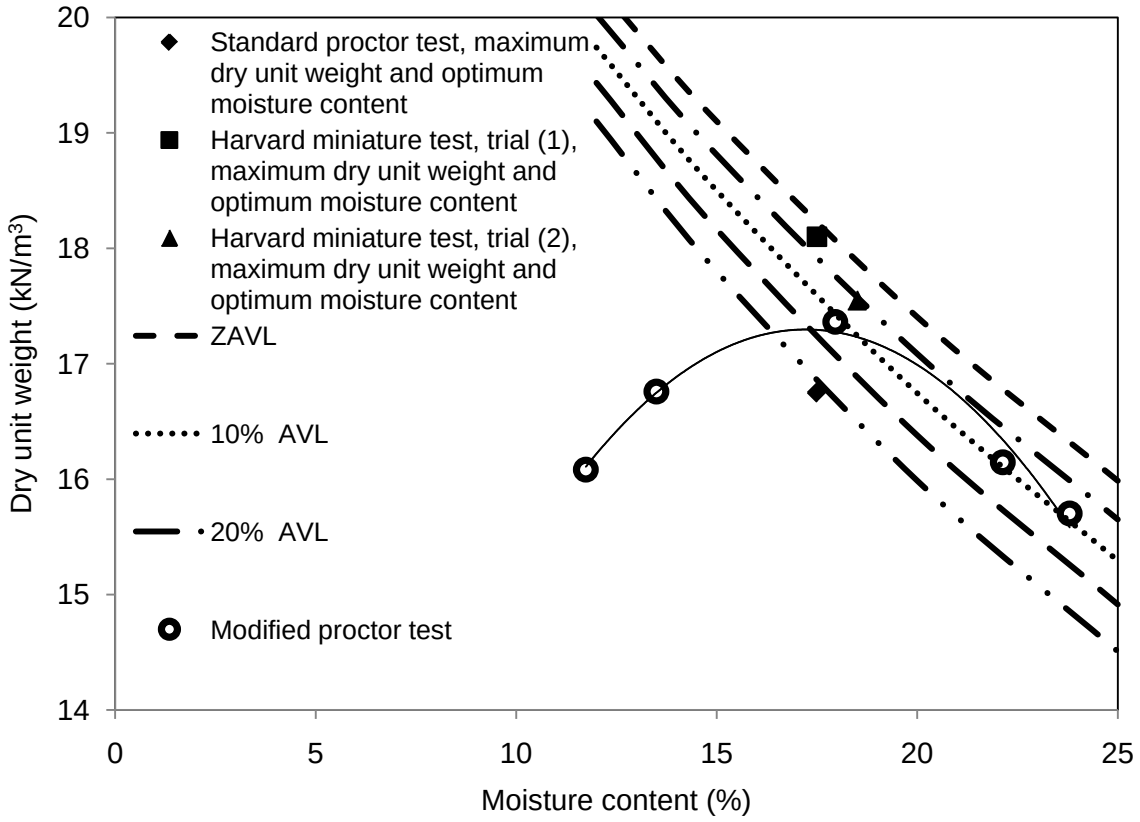


Figure 4. Compaction test results for Chickasha soil

## 3.2. SUCTION SENSORS

In this study, several different methods and sensors were examined to measure the soil suction and moisture content as described in the following sections:

### 3.2.1. FREDLUND SENSORS

The thermal conductivity of a porous medium increases with its moisture content. Therefore, the thermal conductivity of a standard porous (e.g. ceramic) block in equilibrium with the surrounding soil can be used to measure the moisture content of the ceramic block, which in turn, is dependent on the matric suction of the surrounding soil (Pereta et al. 2004). The concept described above makes it possible to calibrate the thermal conductivity of Fredlund sensors against the matric suction in the surrounding soil.

Samples of the Chickasha soil were placed and compacted in a test bucket to examine the performance of our three available Fredlund thermal sensors in measuring soil suction (Fredlund et al. 2000, Pereta et al. 2004). Five tests were carried out using these sensors. For each test, the bucket was filled with a sample of Chickasha soil in three lifts which were compacted to 95% of its maximum dry unit weight similar to the target compaction level in the pullout tests. Once each lift was compacted, a cylindrical core was excavated within the soil to place the Fredlund sensor. The soil was then backfilled around the sensor and compacted (**Figure 5**).

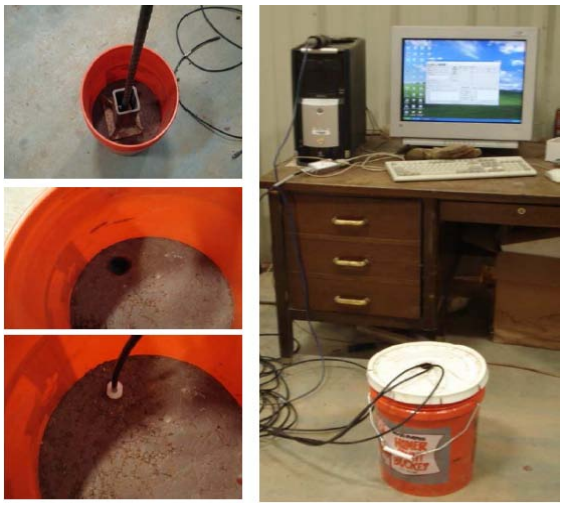

Figure 5. Fredlund sensors placed in a calibration bucket to measure matric suction of the Chickasha soil

The positions of the three sensors in the bucket are schematically shown in **Figure 6.** After taking suction readings and finishing each test, soil samples were taken from the areas around each sensor to measure their moisture content. We waited 24 hours between consecutive readings for sensors to equilibrate with the surrounding soil. This procedure was repeated on the soil placed in the bucket at different moisture content values. The resulting Soil Water Characteristic Curves (SWCC) from Fredlund sensors are plotted in **Figure 7**.

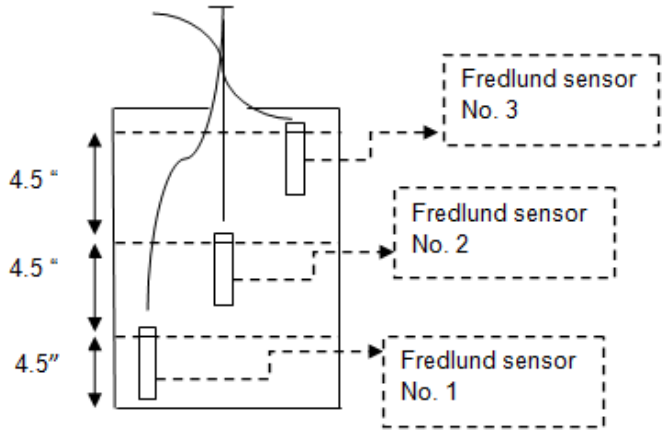


Figure 6. Schematic cutaway section indicating the locations of Fredlund sensors in the calibration bucket

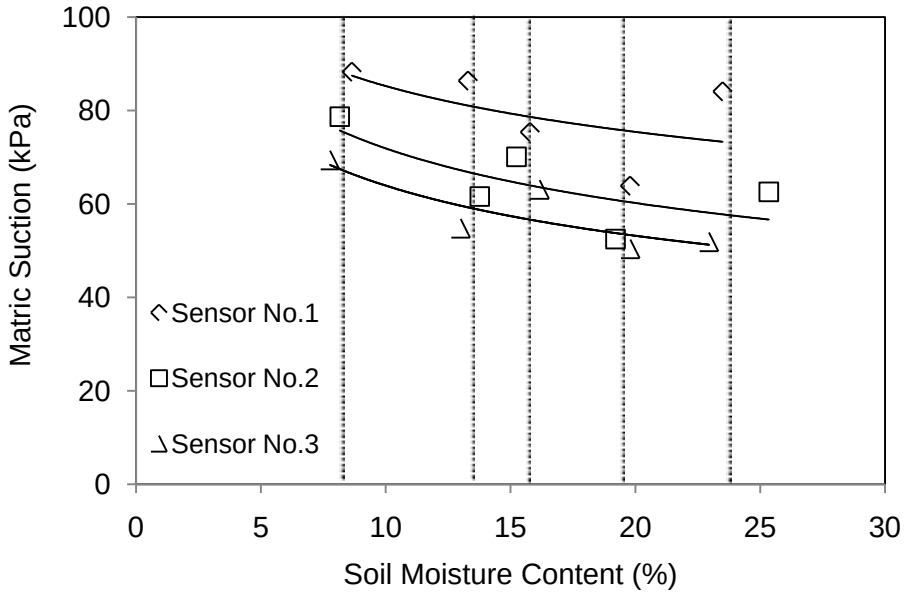


Figure 7. Soil suction versus moisture content for Chickasha soil from Fredlund sensors. Note: The vertical lines indicate the mean values of measured moisture content in each test.

The data in **Figure 7** show a reasonable trend of reduction in the soil suction at higher moisture contents. However, the scatter in data is significant. Moreover, the range of suction values is significantly lower than what is expected for Chickasha soil (i.e. on the order of 1000 kPa on the dry side of optimum) as measured using WP4 equipment (See **Section 3.2.4**). A possible

reason for the above shortcomings is that the Fredlund sensors need to be in complete contact with the backfill soil to function properly. Extra care was taken to compact the soil as best as possible around the sensors after they were placed in the cavities in the calibration bucket. However, due to the small amount of soil that needed to be compacted and space limitations around the sensors, achieving proper compaction without disturbing the intact soil around the hole proved to be challenging. Results in **Figure 7** indicate that readings from these sensors could be very sensitive to the placement procedure. Therefore, it was decided to search for other suction/moisture sensors for this study.

### 3.2.2. PST 55 PSYCHROMETER

PST 55 is an in-situ psychrometer which can measure soil total suctions up to 5000 kPa. Under vapor equilibrium conditions, water potential of its porous cup is directly related to the vapor pressure of the surrounding air. This means that the soil water potential is determined by measuring the relative humidity of the chamber inside the porous cup (Campbell et al. 1971). PST 55 psychrometers are much smaller than Fredlund sensors and are commonly used in geotechnical research projects. PST 55 Psychrometer sensors can lose their factory calibration over time. Therefore, in this study we calibrated them using a 1000 mmol/kg NaCl solution before we used them in the pullout tests. **Figure 8** shows a snapshot of the calibration setup and procedure for these sensors.

(a) (b)

Figure 8. (a) A PST 55 sensor submerged in NaCl solution; (b) Sensor calibration setup

The data logger shown in **Figure 8b** was used to read the water potential of the NaCl solution samples, and the ice chest provided a controlled temperature and moisture environment for the

calibration of the sensors. The sensors were submerged in NaCl solutions and kept in the ice chest for about 2 hours to reach equilibrium (Wescor Inc. 2001). Then, each sensor was connected to the data logger (one at a time) and the water potential of the control NaCl solution was read in microvolts ($\mu V$). Four Psychrometer sensors were calibrated and the results are given in **Table 2**.

Table 2. Summary of PST 55 Psychrometer sensor calibration data using a 1000 mmol/kg NaCl solution (Standard/target water potential: 2500 kPa)

| Sensor # | Temperature (°C) | Sensor output (µv) | Water Potential (kPa) | Calibration factor |
|---|---|---|---|---|
| 1 | 23.9 | 18 | 2400 | 1.04 |
| 2 | 23.9 | 17 | 2270 | 1.10 |
| 3 | 23.9 | 19 | 2530 | 0.99 |
| 4 | 23.9 | 18 | 2400 | 1.04 |

### 3.2.3. FILTER PAPER

In-contact and non-contact filter paper techniques are used to measure the soil matric and total suction values, respectively. In the in-contact filter paper technique, water content of the initially dry filter paper increases due to a flow of water in liquid form from the soil to the filter paper until the two media come into equilibrium with each other. After equilibrium is established, the water content of the filter paper is measured. Then, by using the appropriate filter paper calibration curve, the soil matric suction is estimated. In the non-contact technique, the dry filter paper is suspended above a soil specimen in a sealed container for water vapor equilibrium between the filter paper and the soil specimen at a constant temperature. The vapor space above the soil specimen acts as a true semi-permeable membrane which is only permeable to water vapor but not to ions from the pore-water. The separation between the filter paper and the soil by a vapor barrier limits water exchange to the vapor phase only and prevents solute movement. Therefore, in this technique, the total suction is measured. After equilibrium, the filter paper is removed and water content of the filter paper determined as quickly as possible. Then, by using the appropriate filter paper calibration curve, the soil total suction is estimated (Pan et al. 2010).

Chickasha soil samples were prepared at OMC-2% and OMC+2% moisture contents to predict maximum and minimum suction levels in our pullout tests. The filter paper test method was used as an alternative means to measure the soil matric suction as per the ASTM D5298-10 test standard (ASTM 2010). Each soil sample was cut into two halves with smooth surfaces. A circular piece of Whatman filter paper with the diameter d = 42 mm was placed between two larger papers (d = 55 mm). All three papers were sandwiched between the two soil halves which were then taped together. The entire assembly was placed in a jar. To measure total suction, a piece of geogrid was placed on the top of the taped soil specimen and two large filter papers were placed on the top. The geogrid provided a suitable and convenient way to leave a small gap between the unsaturated soil sample and the filter paper assembly. Next, the jar lid was put back on and labeled with the information on the soil sample. The jar was placed in a well-insulated container for suction equilibrium and its temperature was monitored and recorded. This process was repeated for all other samples. **Figure 9** and **Table 3** show the calibration curve for the filter paper used and the test results, respectively.

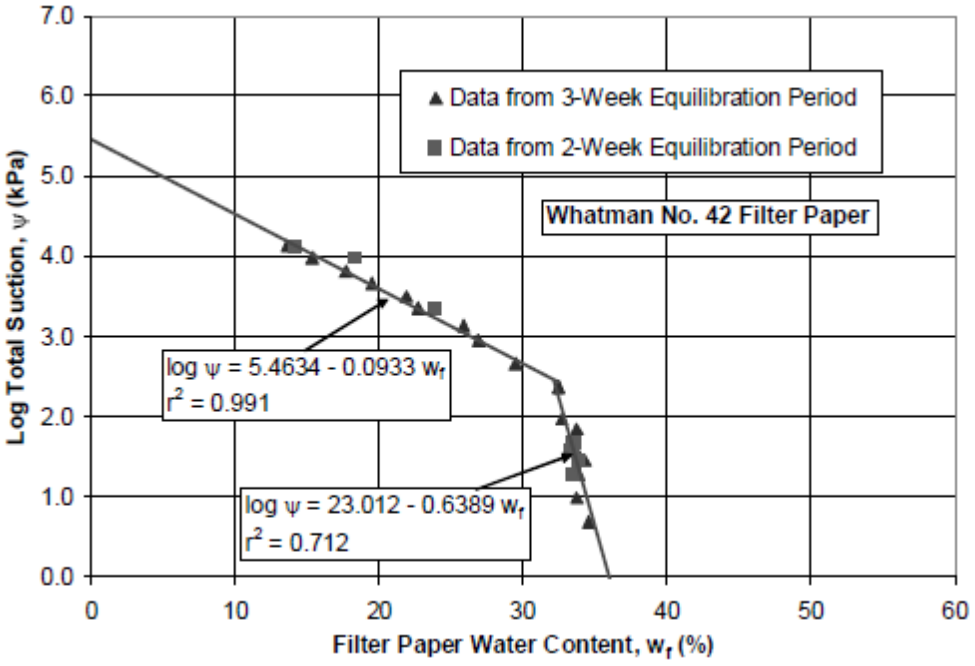


Figure 9. Filter paper calibration curve for Whatman No.42 filter paper (from Chao 2007)

Table 3. Filter Paper test results for Chickasha soil

| Measured Suction | OMC-2% | | | | OMC+2% | | | |
|---|---|---|---|---|---|---|---|---|
| | Top Filter Paper | | Bottom Filter paper | | Top Filter Paper | | Bottom Filter paper | |
| | Test (1) | (2) | Test (1) | (2) | Test (1) | (2) | Test (1) | (2) |
| Log kPa | 4.251 | 4.148 | 4.232 | 3.989 | 3.821 | 3.849 | 3.775 | 3.877 |
| Total Suction (kPa) | 17823 | 14060 | 17060 | 9750 | 6622 | 7063 | 5956 | 7534 |
| Average Total Suction (kPa) | 14673 | | | | 6794 | | | |

Note: Two tests were carried out at each target moisture content (OMC-2% and OMC+2%)

According to **Table 3**, since the difference between the two suction values in the repeat trials of nominally identical samples is less than 0.5 Log kPa (ASTM D5298-10), the results are acceptable and no results should be discarded. Therefore, the mean value of total suction for each of the OMC-2% and OMC+2% cases for the Chickasha soil is given in the last row of **Table 3**. Results of **Table 3** are plotted in **Figure 10**.

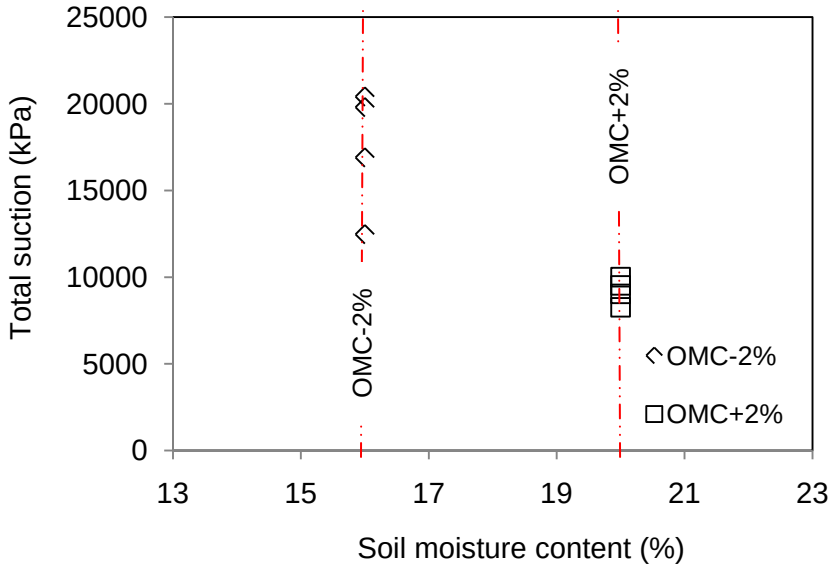


Figure 10. Variation of moisture content and total suction for Chickasha soil from filter paper tests

Although the results in **Figure 10** show a reasonable trend of lower total suction at higher moisture content values, the measured values of total suction for Chickasha soil are significantly higher than what is expected (see **Section 3.2.4**). There are three critical parameters that must be considered in order to achieve reasonable results from filter paper tests. First, this test method requires an extremely clean lab environment. Second, the test should be carried out at constant temperature and relative humidity. Third, the weights of the filter papers need to be measured immediately after the samples reach equilibrium. Failure to adhere to any one of these requirements could result in significant errors in the measured results.

### 3.2.4. WP4 POTENTIOMETER

The WP4 equipment measures the soil total suction. It consists of a sealed block chamber equipped with a sample cup, a mirror, a dew point sensor, a temperature sensor, an infrared thermometer and a fan (**Figure 11**). The soil sample is placed in the sample cup and brought to vapor equilibrium with the air in the headspace of the sealed block chamber. At equilibrium, the water potential of the air in the chamber is the same as the water potential or suction of the soil sample.


Figure 11. WP4 Water Potentiometer equipment (soil samples in sealed cups are shown in the inset)

Seventeen (17) 300-gram samples of Chickasha soil were prepared at different moisture content values. Approximately 100 grams of each sample was used to measure its moisture content using the oven-drying method. The rest of the soil was used to make a 1.57 inch (diameter) by 0.24 inch (height) sample for the WP4 equipment at the same dry unit weight as was used in the laboratory pullout tests. The WP4 samples were placed in sealed disposable cups (**Figure 11**). Before testing each soil sample using WP4, a salt solution of known water potential (0.5 molal KCl in $H_2O$) was used to calibrate the WP4 sensor. For each test, the sample was placed inside the WP4 sample drawer and was allowed to reach temperature equilibrium with the equipment internal chamber. Then, the knob on the tray was turned to the "READ" position to read the water potential of the soil sample. The magnitude of the soil total suction was recorded once the displayed reading stabilized at a constant value. **Figure 12** shows the Soil-Water Characteristic Curve (SWCC) for Chickasha soil that was obtained through WP4 tests.

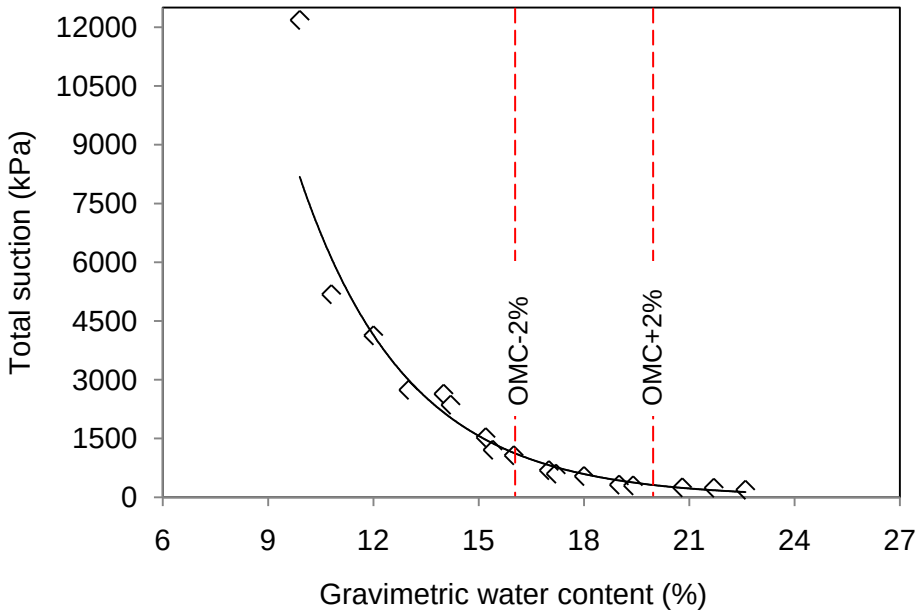


Figure 12. Soil-Water Characteristic Curve for Chickasha soil using WP4 Potentiometer

Results shown in **Figure 12** indicate that the total suction in Chickasha soil varies between 300 kPa and 1200 kPa for the range of moisture contents between OMC-2% and OMC+2%. This range of soil suction is consistent with the values that can be found in the literature for lean clay (Cardoso et al. 2007, Nam et al. 2009).

Analysis of WP4 results also allowed us to determine whether or not Chickasha soil is classified as an expansive clay. For this purpose, a procedure called McKeen analysis was used. In the McKeen's classification methodology for expansive soils the slope of the SWCC in a semi-log plot is used to determine a parameter called the ''total suction-water content index''. The swelling potential of expansive soils is qualitatively classified (e.g. ''low'' or ''high'') based on the magnitude of the total suction-water content index (**Table 4**) (McKeen 1992). **Figure 13** shows a plot of the gravimetric moisture content vs. total suction for the Chickasha soil.

Table 4. Summary of McKeen (1992) Expansive Soil Classification Methodology

| Category | Slope | $c_h$ | $H_c$ (%) | Expansion |
|---|---|---|---|---|
| I | > 0.17 | -0.027 | 10 | Special case |
| II | 0.1 – 0.17 | -0.227 to -0.12 | 5.3 | High |
| III | 0.08 – 0.1 | -0.12 to -0.04 | 1.8 | Moderate |
| IV | 0.05 – 0.08 | -0.04 to 0 | - | Low |
| V | < 0.05 | 0 | - | Non-Expansion |

Note: $c_h$ and $H_c$ are the suction-compression index and vertical movement, respectively as computed by McKeen (1992).

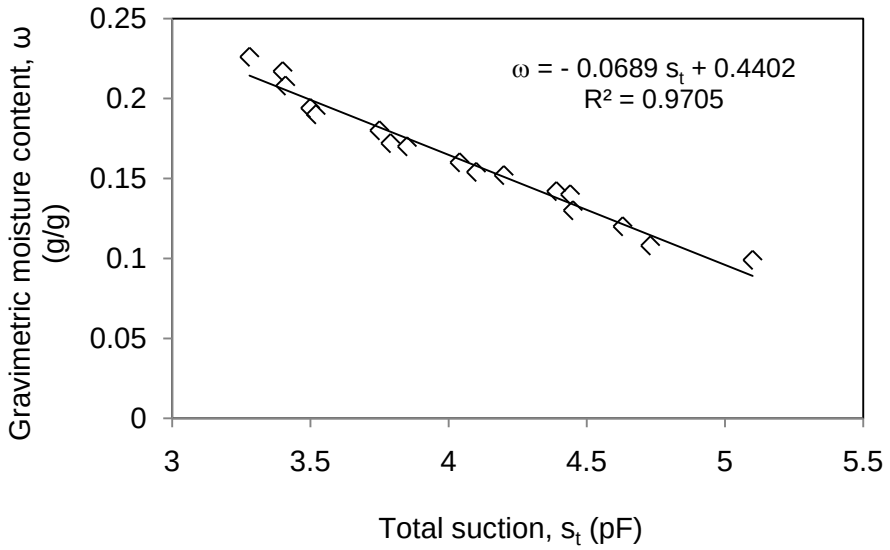


Figure 13. Gravimetric moisture content vs. total suction for Chickasha soil on semi-log plot (pF is the base 10 logarithm of the suction expressed in cm of water)

According to **Table 4** and **Figure 13** since the slope of the graph is less than 0.08, Chickasha soil is classified under category IV indicating that its expansive tendency is low.

Based on our experience with different methods of determining the soil suction as described earlier in this section, we found psychrometers to be the most suitable for in-situ testing and WP4 as the most suitable laboratory equipment to determine the soil suction in this study.

### 3.3. GEOSYNTHETIC REINFORCEMENT

A woven polypropylene (PP) geotextile (Mirafi HP370) was used in the pullout tests carried out in this study. The mechanical response of the geotextile was found as per the ASTM D4595 test protocol (ASTM 2009) and was compared with the manufacturer's data (**Figure 14**, Hatami et al. 2010a).

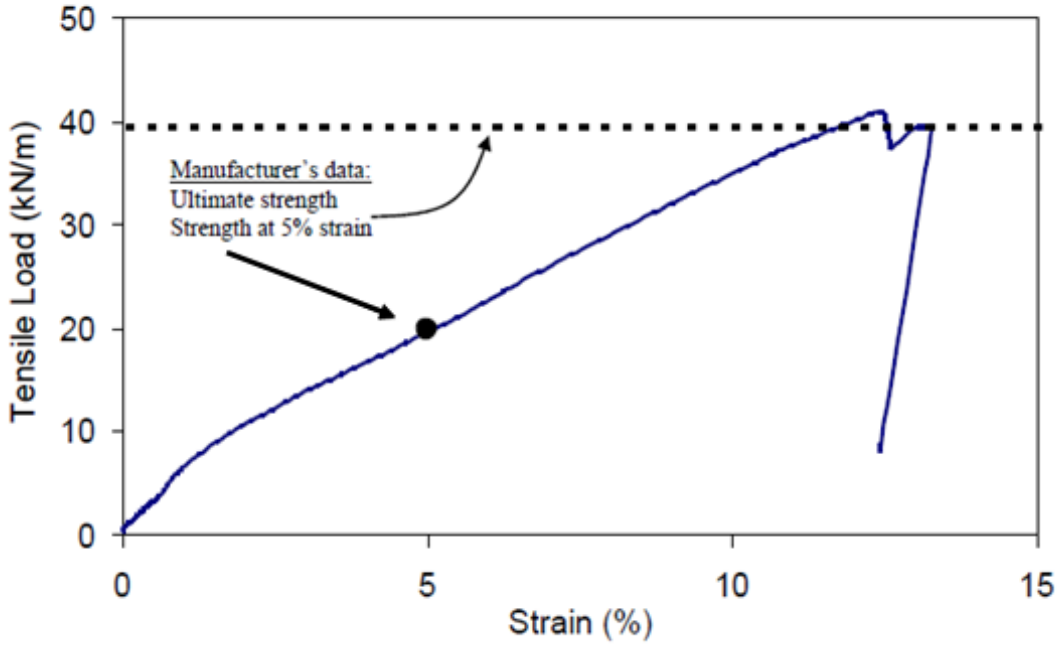


Figure 14. Mechanical response of the geotextile used in the pullout tests (Mirafi HP370) as per the ASTM D4595 test protocol and as compared with the manufacturer's data. Note: two arrows show the ultimate tensile strength and strength of geotextile reinforcement at 5% strain.

# 4. LARGE-SCALE PULLOUT TESTS

## 4.1. METHODOLOGY

A series of large-scale pullout tests were carried out in Chickasha soil and Mirafi HP370 woven geotextile (**Section 3.3**). These tests were carried out at three different moisture content values OMC-2%, OMC and OMC+2% (**Table 5**). The differences in the magnitude of geotextile pullout resistance among these cases were used to determine a moisture reduction factor (MRF = $\mu(\omega)$) in **Equation 1** to account for the loss of reinforcement pullout resistance due to increased moisture content. The tests for each moisture content value were carried out at three different overburden pressures as given in **Table 5**.

Table 5. Large-scale pullout test parameters

| Test information | |
|---|---|
| Soil | Chickasha soil |
| Geosynthetic reinforcement | Mirafi HP370, woven PP |
| Overburden pressure, kPa (psf) | 10 (207), 20 (417.7), 50 (1044.3) |
| Moisture content | OMC-2%, OMC, OMC+2% |

### 4.1.1. TEST EQUIPMENT

The nominal dimensions of the large-scale pullout test box used in this study (**Figure 15**) are 1800 mm (L) × 900 mm (W) × 750 mm (H). The size of the box and its basic components, including metal sleeves at the front end exceed the minimum requirements of the ASTM D6706 test protocol (ASTM 2010). The boundary effects were further minimized by lining the walls of the test box with plastic sheets. The large pullout test equipment has a 4" bore, 18" stroke hydraulic cylinder with a high precision servo-control system. A surcharge assembly including an airbag and reaction beams on the top of soil surface is used to apply overburden pressures up to about 50 kPa (i.e. approximately 1050 psf, or equivalent to 2.5 m of overburden soil) on the soil-reinforcement interface. The pullout load on the reinforcement specimen is applied

using a 90 kN (20 kip), servo-controlled hydraulic actuator. In the tests carried out in this study, only one half of the box length (i.e. 900 mm) was used.

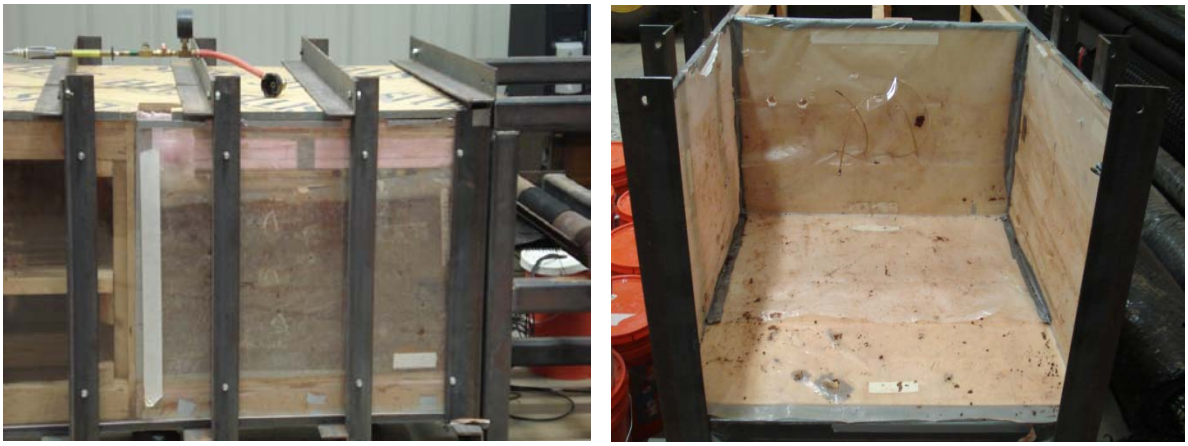

Figure 15. One of the pullout test boxes at the OU Fears laboratory

### 4.1.2. INSTRUMENTATION

Different instruments were used to measure the movement of geotextile reinforcement and soil suction near the soil-geotextile interface in the pullout tests. A set of PST 55 Psychrometer sensors was placed in rows above and below the soil-geotextile interface to measure the soil suction and moisture content near the soil-reinforcement interface (**Section 4.2**).

The geotextile strains and local displacements were measured using four (4) wire-line extensometers attached to different locations along the reinforcement length (**Figure 16a**). A Geokon Earth Pressure Cell (EPC) was used to verify the magnitude of the overburden pressure applied on the soil-geotextile interface using the airbag that was placed on the top of the soil (**Figure 16b**). **Figure 17** shows the strain distributions over the length of geotextile reinforcement at maximum pullout force at the points to which wire-line extensometers were attached. The strain near the front end of the geotextile reinforcement was calculated using the displacements at the front end of the geotextile and at the location of extensometer 1. The former value was determined by subtracting the calculated elongation of the in-air portion of the geotextile specimen from the actuator displacement. Results in **Figure 17** indicate that strains in the geotextile reinforcement are greater at higher overburden pressures and lower soil moisture content values (i.e. higher soil suction).

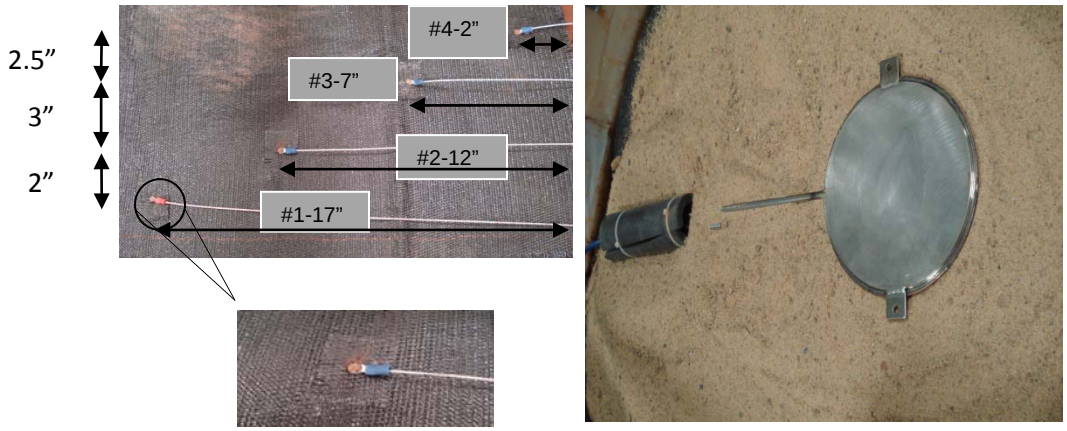


(a) (b)

Figure 16. (a) Wire-line extensometers attached to the geotextile reinforcement (the numbers in the figure indicate the extensometer number and distance from the tail end of the geotextile); (b) Earth pressure cell placed on the top of the soil in the pullout test box

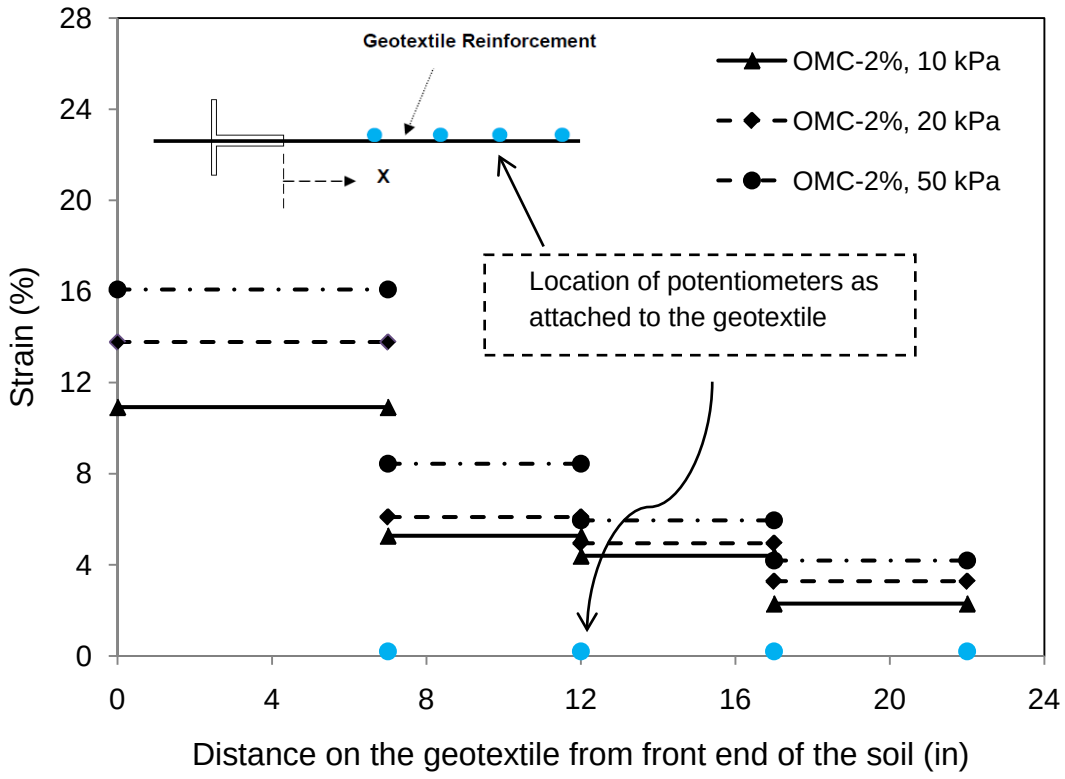


(a)

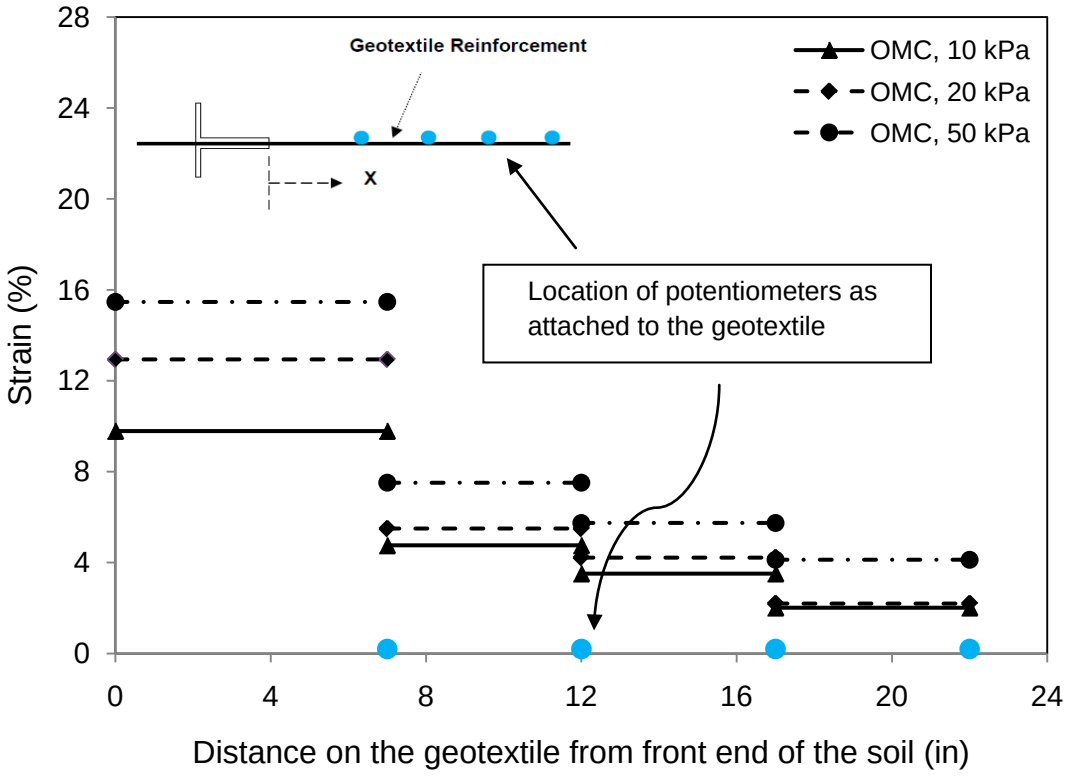
Geotextile Reinforcement
X
OMC, 10 kPa
OMC, 20 kPa
OMC, 50 kPa
Location of potentiometers as attached to the geotextile
Strain (%)
0
4
8
12
16
20
24
28
Distance on the geotextile from front end of the soil (in)

(b)

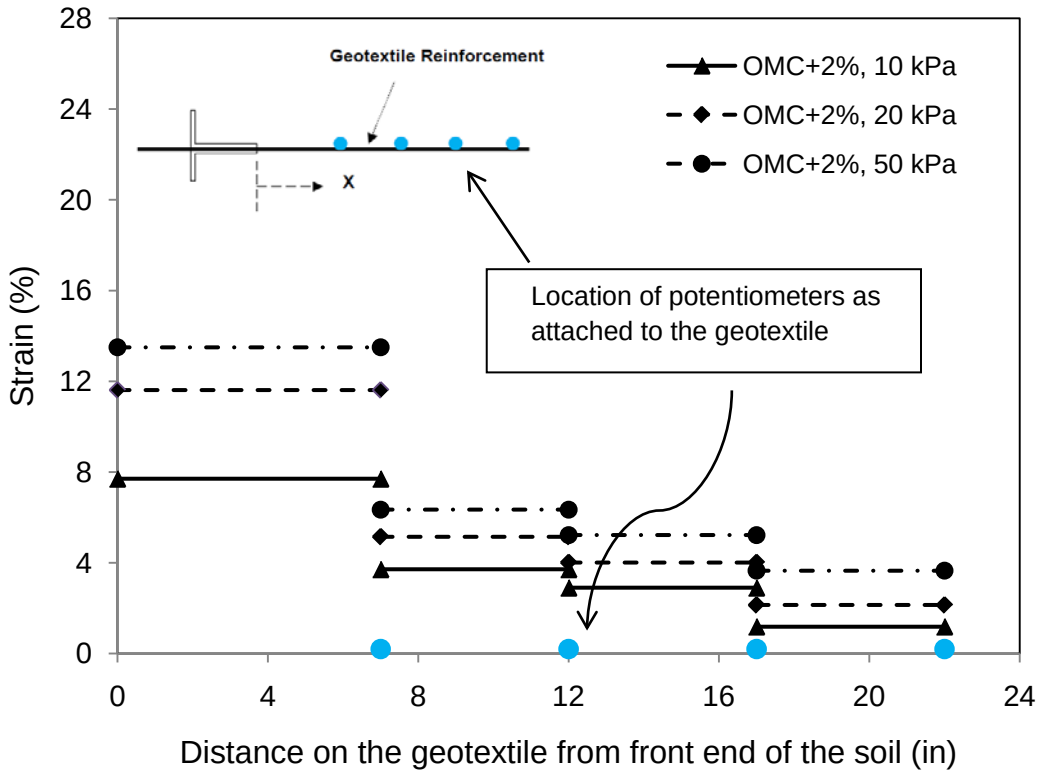
Geotextile Reinforcement
X
OMC+2%, 10 kPa
OMC+2%, 20 kPa
OMC+2%, 50 kPa
Location of potentiometers as attached to the geotextile
Strain (%)
0
4
8
12
16
20
24
28
Distance on the geotextile from front end of the soil (in)

(c)

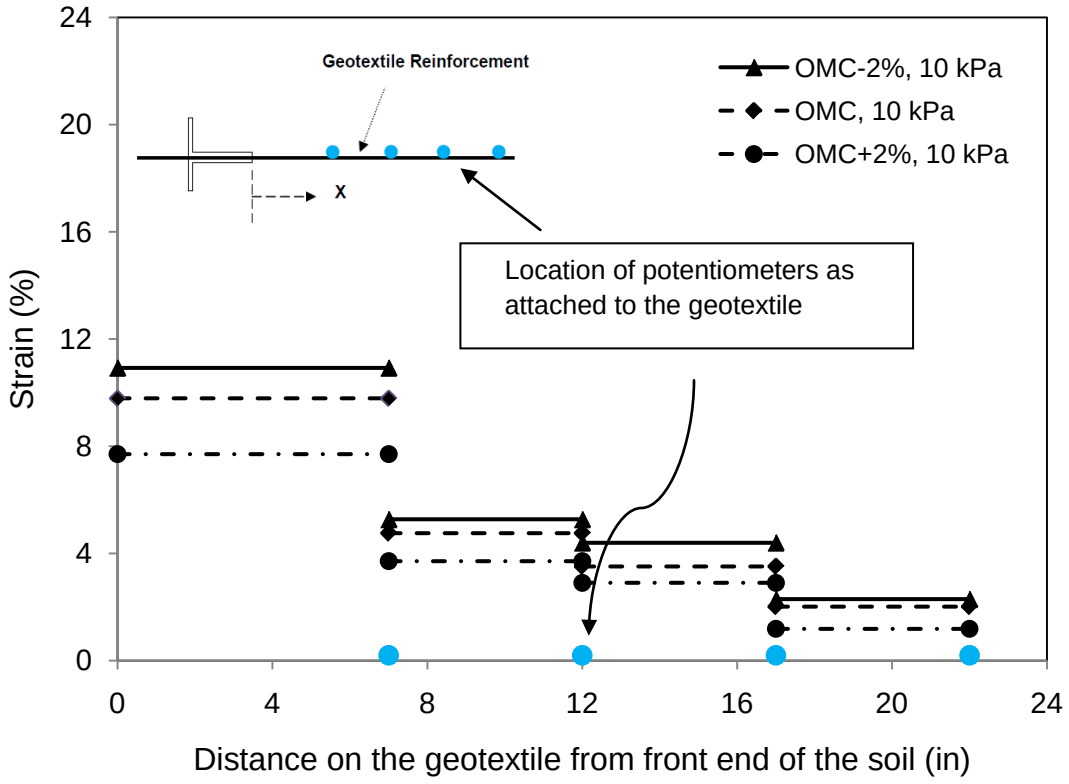
Geotextile Reinforcement
X
OMC-2%, 10 kPa
OMC, 10 kPa
OMC+2%, 10 kPa
Location of potentiometers as attached to the geotextile
Strain (%)
0
4
8
12
16
20
24
Distance on the geotextile from front end of the soil (in)

(d)

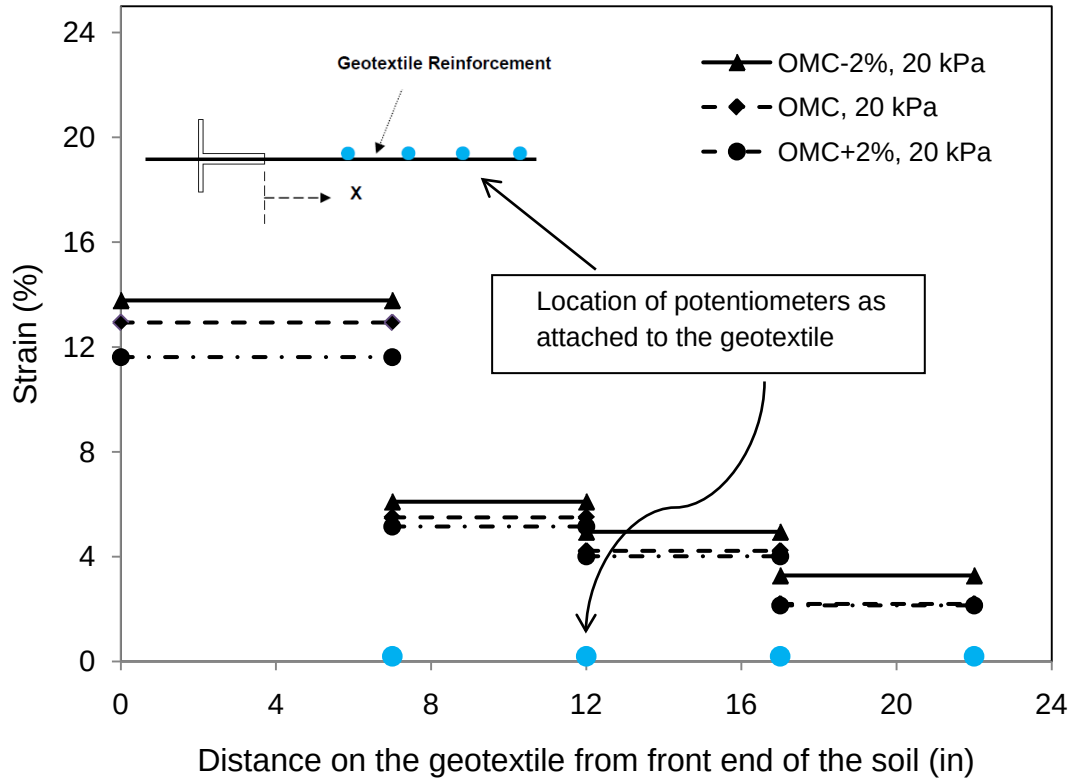
Geotextile Reinforcement
X
OMC-2%, 20 kPa
OMC, 20 kPa
OMC+2%, 20 kPa
Location of potentiometers as attached to the geotextile
Strain (%)
0
4
8
12
16
20
24
Distance on the geotextile from front end of the soil (in)

(e)

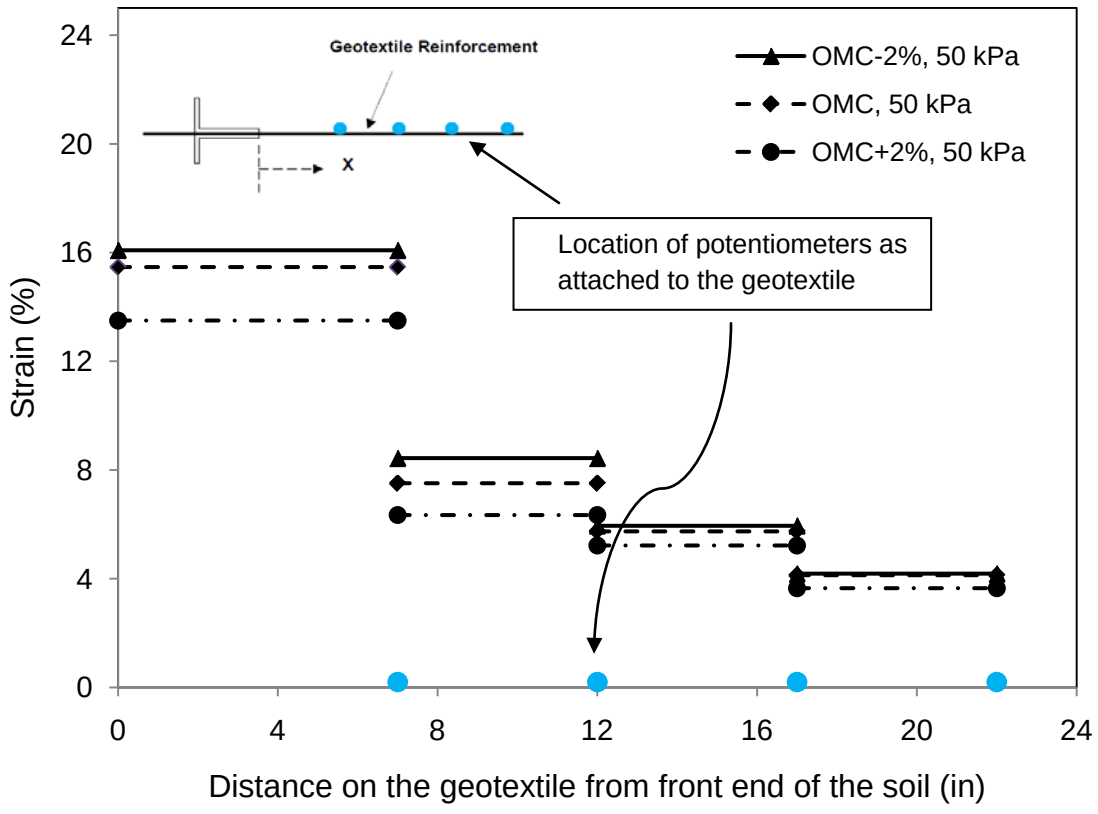


(f)

Figure 17. Axial strain distribution over the length of geotextile reinforcement from large-scale pullout test on Chickasha soil at different moisture contents and overburden pressures

## 4.2. TEST PROCEDURE

### 4.2.1. PROCESSING OF THE SOIL

After the soil was transported from the borrow site (**Figure 2**) to the Fears lab, the clayey soil was air dried and broken into small pieces using two soil processors (**Figures 18a,b**). Afterwards, the soil was passed through a #4 sieve in a 7-tray Gilson screen shaker. Next, the soil was mixed with water to reach the desired moisture content for each test (**Figure 18c**). This procedure took approximately 5 to 7 days depending on the initial soil moisture content. The wet soil was stored in thirty five to forty 25 kg (55 lb)-buckets and was sealed for more than 24 hours to reach moisture equilibrium. The soil moisture content in each bucket was measured using the oven drying method (**Figure 19**). The above procedure was repeated for every test.

(a)


(b)

(c)

Figure 18. Soil processing equipment at the OU Fears laboratory, (a, b) Soil processors, (c) Soil mixer

(a) (b)

Figure 19. (a) Sealed buckets containing processed soil before placing in the pullout box, (b) Soil samples in the oven to determine their moisture content

### 4.2.2. PLACEMENT OF THE SOIL IN THE PULLOUT BOX

The pullout box was lined with plastic sheets to preserve the soil moisture content and to minimize the friction between the soil and the sidewalls during each test. Next, the soil was placed and compacted in the test box in nine two-inch lifts. The soil was compacted to 95% of its maximum dry unit weight (i.e. $\gamma_d$ = 16.44 kN/m$^3$ = 104.6 pcf). The compaction for each layer took approximately 1 hour. The instrumented geotextile was placed at the mid-height of the box. The pullout box containing compacted soil at its target moisture content was sealed with plastic sheets on the top (**Figure 20**).

(a) (b)

Figure 20. (a) Sealed compacted soil at the end of large-scale pullout box setup, (b) Geotextile specimen at the mid-height of the pullout box

The soil was left for at least 24 hours until the Psychrometer sensors reached equilibrium with their surrounding soil. In all pullout tests, a rectangular block of Styrofoam with dimensions 900 mm (W), 457 mm (H) and 140 mm (T) was used in front of the soil specimen, which in addition to the 200 mm-wide metal sleeves, helped further minimize the influence of front boundary condition on the soil-geotextile interface.

### 4.2.3. PULLOUT TEST AND DISMANTLING OF THE TEST SETUP

The pullout phase of the test usually took between 1 and 2 hours depending on the overburden pressure and target soil moisture content. The pullout force was applied on the geotextile reinforcement at a target displacement rate of 1 mm/min according to the ASTM D6706 test protocol. After the test was completed and the reinforcement underwent pullout failure, the test assembly was carefully dismantled. First, the surcharge assembly was removed from the top of the box and the soil was carefully excavated from the box. It usually took about 4 to 5 hours to carefully dig the entire soil out of the test box. All together, a complete test required 45 to 50 hours of hands-on operation including soil processing, mixing and setting up the box, 24 to 48 hours as equilibrium time for suction sensors and 1 to 2 hours to run the pullout test. **Figure 21** shows a schematic diagram of the pullout box. In this figure, the white circles represent the locations of samples that were taken to measure the soil suction with the WP4 Potentiometer and the black circles show the locations of the in-situ PST 55 Psychrometer sensors.

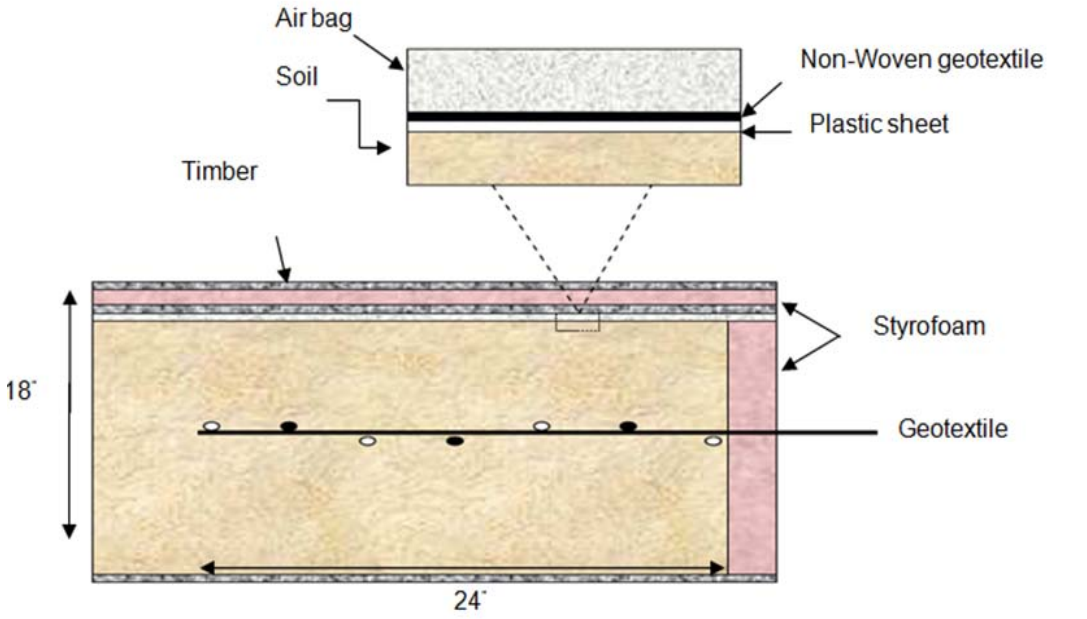


Figure 21. Schematic diagram of the large-scale pullout box test setup

### 4.2.4. INTERFACE PROPERTIES

**Figures 22 and 23** show the pullout test data and interface shear strength results for Chickasha soil for different moisture content and overburden pressure values. The nominal moisture content values include OMC-2% (16%), OMC (18%) and OMC+2% (20%). The measured pullout force is plotted as a function of the actuator displacement. Maximum pullout forces on each graph are indicated using hollow circular markers. Results shown in **Figure 22** indicate that reinforcement pullout resistance increases with overburden pressure. Results in **Figure 23** show consistently higher maximum reinforcement pullout resistance in the soil at OMC-2% compared to the values in the OMC and OMC+2% cases for all overburden pressure magnitudes tested. As expected, increasing suction led to a higher maximum reinforcement pullout resistance in otherwise identical test specimens (**Figure 22d**). The interface strength parameters shown in **Figure 22d** are defined in **Equation 2** (**Section 2.2**). Results shown in **Figure 22d** indicate that the interface friction angle does not change with moisture content, whereas the adhesion increases at lower moisture content due to higher suction. This observation is consistent with those reported by Khoury et al. (2011) from suction-controlled interface testing of fine-grained soil specimens.

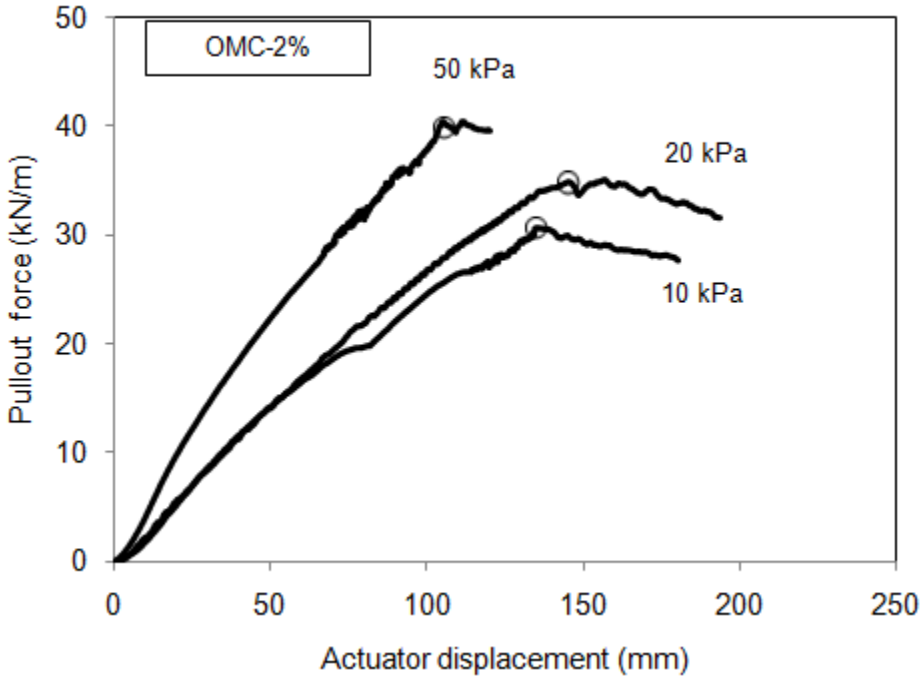


(a)

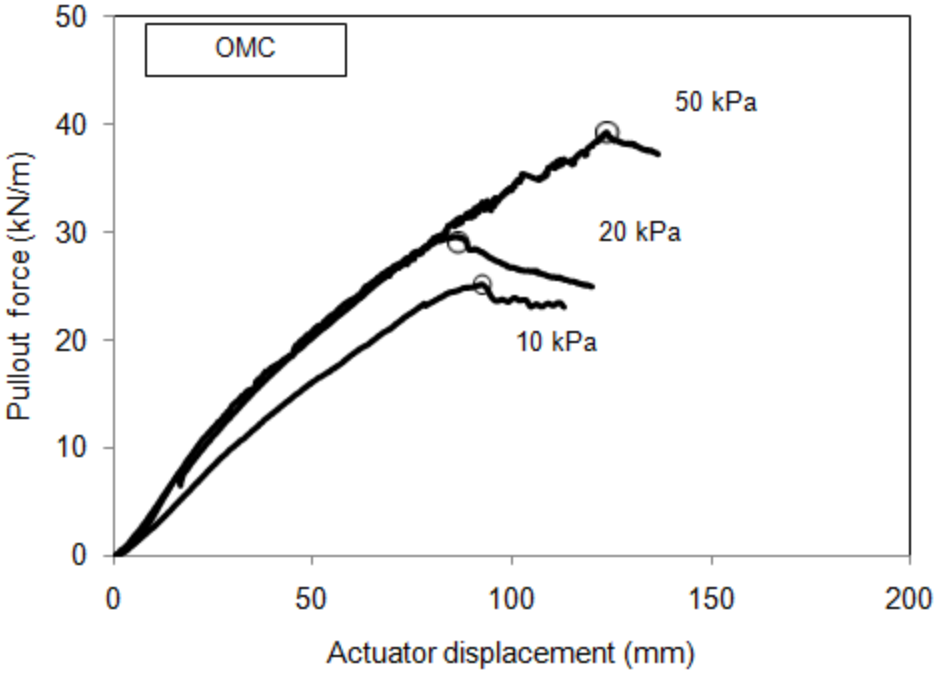
OMC
50 kPa
20 kPa
10 kPa
Pullout force (kN/m)
Actuator displacement (mm)
0
10
20
30
40
50
0
50
100
150
200

(b)

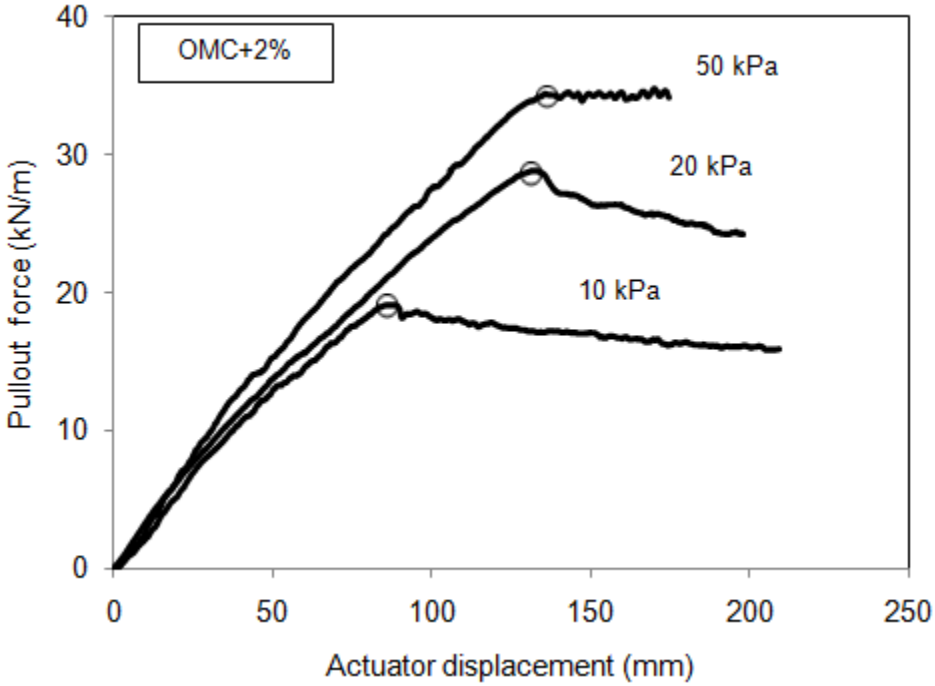
OMC+2%
50 kPa
20 kPa
10 kPa
Pullout force (kN/m)
Actuator displacement (mm)
0
10
20
30
40
0
50
100
150
200
250

(c)

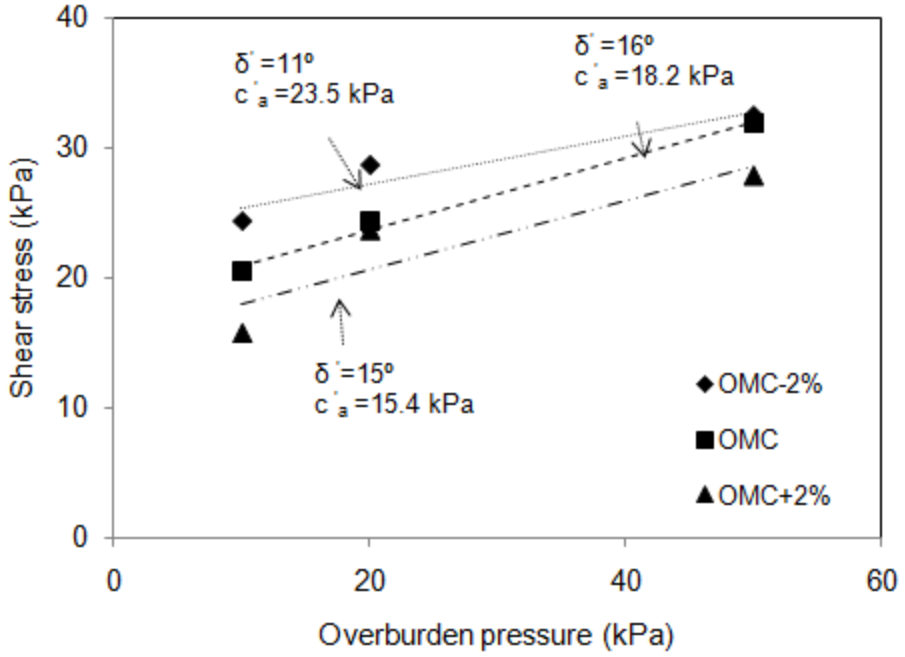


(d)

Figure 22. Pullout test data and interface strength results for Chickasha soil and comparison of failure envelopes for soil-geotextile interface at different moisture content values (OMC-2%, OMC, OMC+2%).

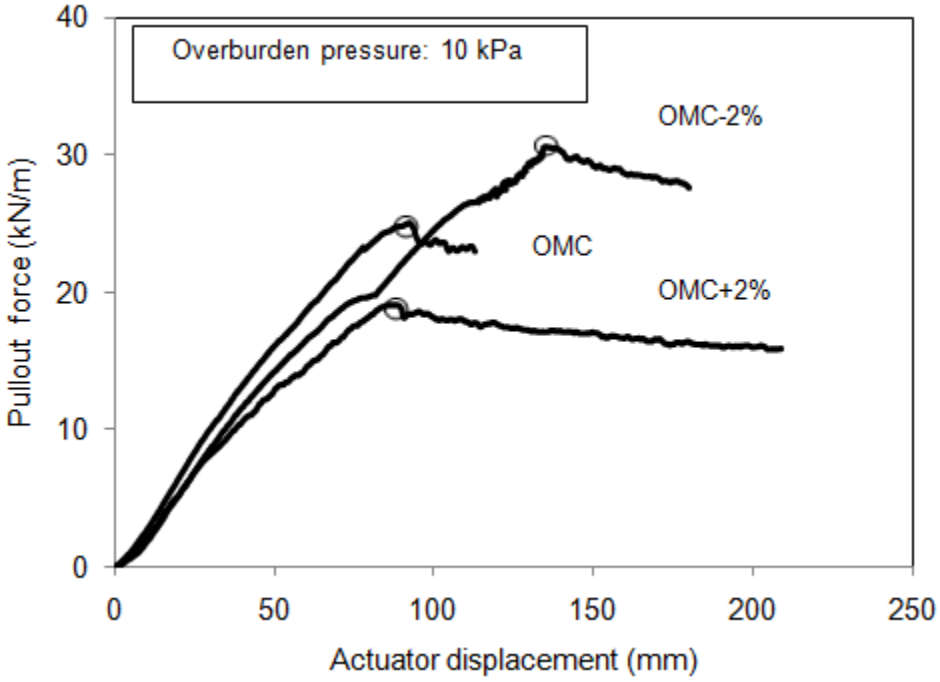


(a)

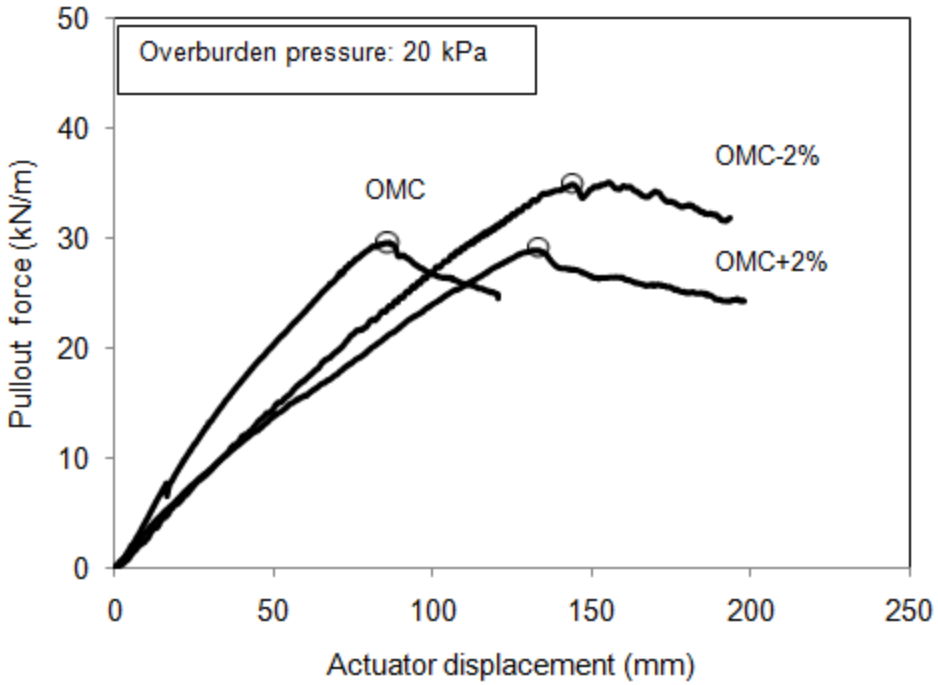


(b)

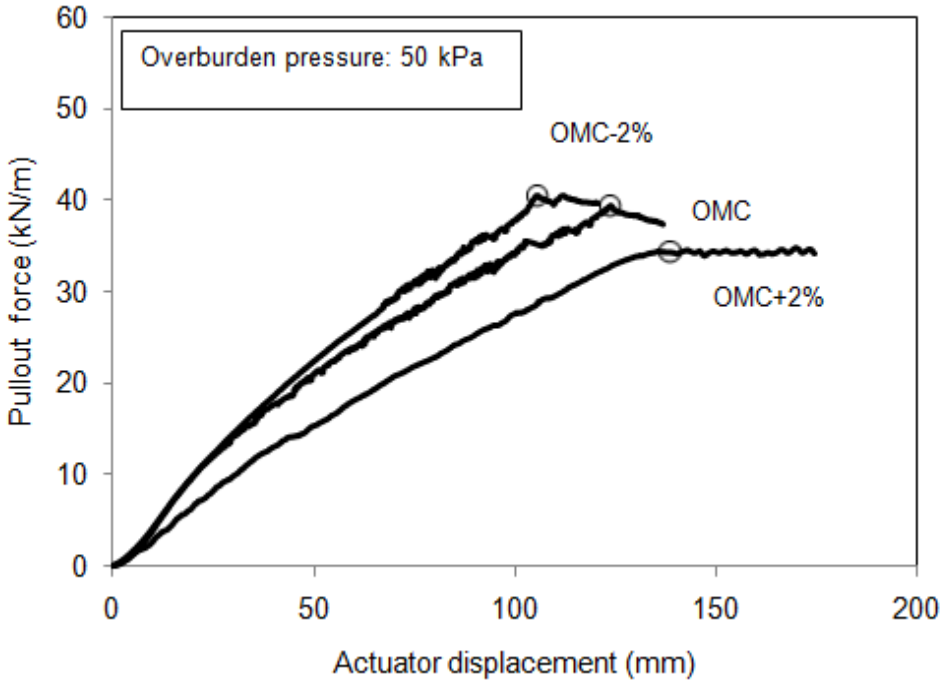


(c)

Figure 23. Pullout test data for Chickasha soil at different overburden pressure values

Results of **Figures 22 and 23** are plotted with respect to the actuator displacement and therefore include the elongation of the in-air portion of the geotextile reinforcement outside the large-scale pullout box. **Figure 24** shows a comparison between the actuator and the geotextile front end displacements for the pullout test at OMC-2% subjected to 50 kPa overburden pressure. The displacement of the geotextile front end (inside the soil) was determined by subtracting calculated values of in-air geotextile elongation (using the mechanical response of the geotextile given in **Figure 14**) from the clamp displacement. Results shown in **Figure 24** indicate that the 0.38-m in-air portion of the geotextile stretched 42.7 mm when subjected to the maximum pullout load.

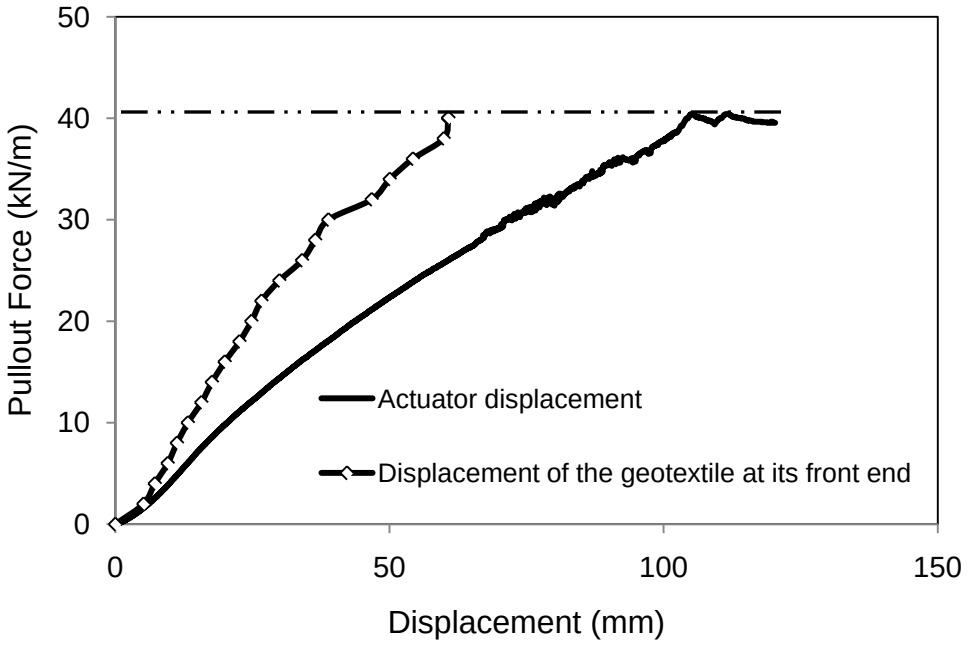


Figure 24. Comparison between the actuator and the geotextile front end displacements for the pullout test at OMC-2% subjected to 50 kPa overburden pressure. Note: The horizontal dashed line shows the maximum pullout force.

Results shown in **Figure 22** represent the frontal planes of extended Mohr-Coulomb failure envelopes for the soil-geotextile interface at different moisture content and suction values. These failure envelopes can be considered to be practically linear for all moisture content cases examined (i.e. OMC-2%, OMC and OMC+2%). The interface strength results, i.e. the values for the slope (tan $\delta$') and the intercept ($c'_a$) of the failure envelopes on these frontal planes are summarized in **Table 6**. Abu-Farsakh et al. (2007) studied the effect of soil moisture content on the interaction between three cohesive soils and a woven geotextile reinforcement material. They found that an increase in the molding moisture content of the soil from 24% to 33%

caused 43 % reduction in the interface shear resistance. The data summarized in **Table 6** are overall consistent with Abu-Farsakh et al.'s observations.

Table 6. Interface strength properties from pullout tests in Chickasha soil

| Target ω (%) | $\sigma_n$ (kPa) (psf) | Mean ω (%)[1] | Mean Ψ (kPa) [2] | $P_r$ (kN/m) | $\tau_{max}$ (kPa) | $\delta'$ (º) | c'$_a$ (kPa) |
|---|---|---|---|---|---|---|---|
| 16 (OMC-2%) | 10 (208) | 16.0 | 1153 | 29.6 | 24.3 | | |
| | 20 (417.7) | 16.0 | 1151 | 34.8 | 28.6 | 11 | 23.5 |
| | 50 (1044.3) | 16.0 | 1135 | 39.4 | 32.4 | | |
| 18 (OMC) | 10 (208) | 18.3 | 550 | 24.8 | 20.4 | | |
| | 20 (417.7) | 18.2 | 566 | 29.7 | 24.4 | 16 | 18.2 |
| | 50 (1044.3) | 18.1 | 576 | 38.7 | 31.8 | | |
| 20 (OMC+2%) | 10 (208) | 20.3 | 286 | 19.1 | 15.7 | | |
| | 20 (417.7) | 20 | 312 | 28.8 | 23.7 | 15 | 15.4 |
| | 50 (1044.3) | 20.2 | 290 | 33.8 | 27.8 | | |

Notes: [1] Mean values were calculated using 45 moisture content samples for each pullout test (5 samples from each of the nine 2-inch soil lifts); [2] Mean values were determined from SWCC for Chickasha soil (**Figure 12**) based on the mean moisture content value determined for each test (i.e. out of 45 data points).

**Figure 25** shows local displacements of the geotextile at the four contact points with the wire-line extensometers as shown in **Figure 16**. The data show a consistent and successive mobilization of the reinforcement strength from the front end (EX1) to the tail end (EX4) of the geotextile specimen until pullout.

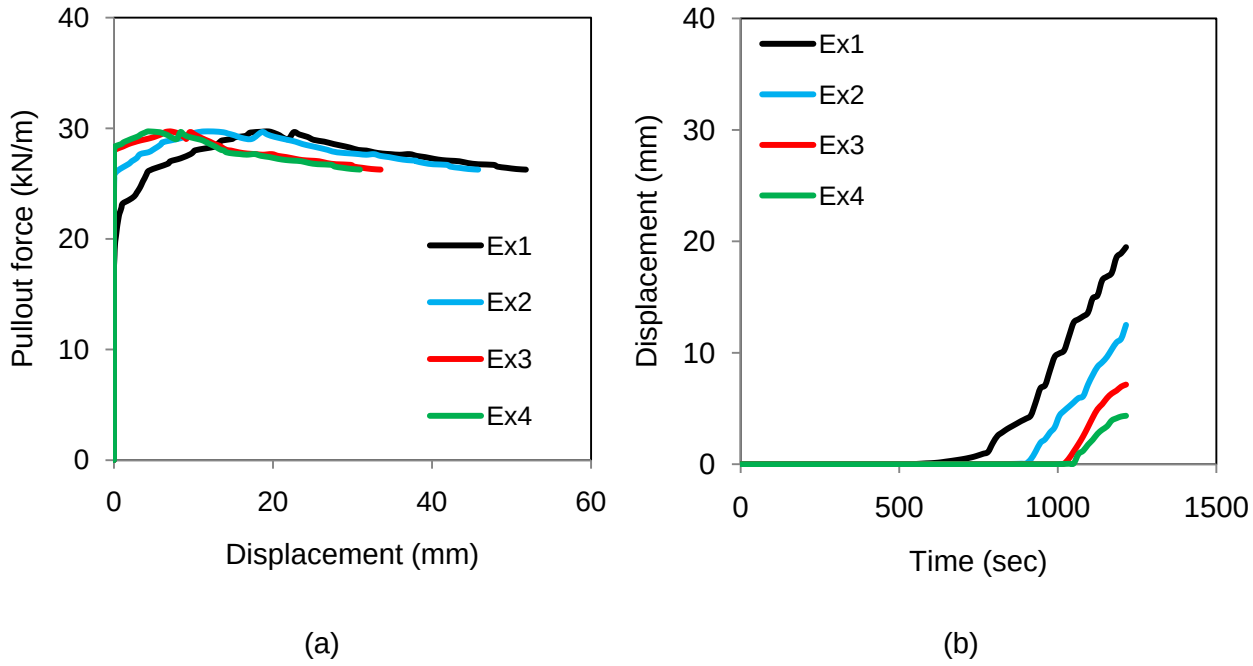


Figure 25. Local displacements of the geotextile reinforcement in a large-scale pullout test at OMC subjected to 20 kPa overburden pressure

### 4.2.5. SOIL MOISTURE CONTENT AND SUCTION

**Figures 26 and 27** show the distributions of soil moisture content and total suction in each layer for all large-scale pullout tests carried out in this study. The mean and Coefficient of Variation (COV) values for these parameters were calculated for the fifth layer (lift) in the pullout box (i.e. for the soil layer on which the geotextile reinforcement was placed) to examine how close the as-placed values were to the target values. **Table 7** shows the mean and Coefficient of Variation values for moisture content and total suction at the fifth layer in large scale pullout tests.

Table 7. Mean and COV values for the fifth layer (in contact with geotextile) in large scale pullout tests

| Target ω (%) | $\sigma_n$ (kPa) (psf) | Mean Ψ (kPa) | $COV_{(\Psi)}$ (%) | Mean ω (%) | $COV_{(\omega)}$ (%) |
|---|---|---|---|---|---|
| 16 (OM-2%) | 10 (208) | 1236 | 7.3 | 15.7 | 1.5 |
| | 20 (417.7) | 1196 | 5.9 | 15.8 | 1.1 |
| | 50 (1044.3) | 1125 | 3.4 | 16 | 0.7 |
| 18 (OMC) | 10 (208) | 513 | 5.7 | 18.5 | 0.9 |
| | 20 (417.7) | 570 | 6.7 | 18.1 | 1.1 |
| | 50 (1044.3) | 590 | 8.2 | 18 | 1.5 |
| 20 (OMC+2%) | 10 (208) | 304 | 11.2 | 20.1 | 1.8 |
| | 20 (417.7) | 352 | 9.9 | 19.6 | 1.6 |
| | 50 (1044.3) | 298 | 11 | 20.1 | 1.7 |

The accuracy of the soil suction values from the PST 55 Psychrometers was examined by comparing them with the readings from the WP4 Potentiometer as shown in **Table 8**. Recall that **Figure 21** shows the locations of the Psychrometer sensors and WP4 samples inside the large-scale pullout box.

Table 8. Comparison of total suction values in Chickasha soil as measured using Psychrometer (in-situ) and WP4 (offsite equipment)

| Target moisture content (%) | Total Suction (kPa) | | |
|---|---|---|---|
| | PST 55 Psychrometers | WP4 | Difference (%) |
| OMC-2% | 910 | 1135 | 25 |
| OMC | 520 | 570 | 10 |
| OMC+2% | 310 | 282 | 9 |

Note: each reported value is the mean value of three samples.

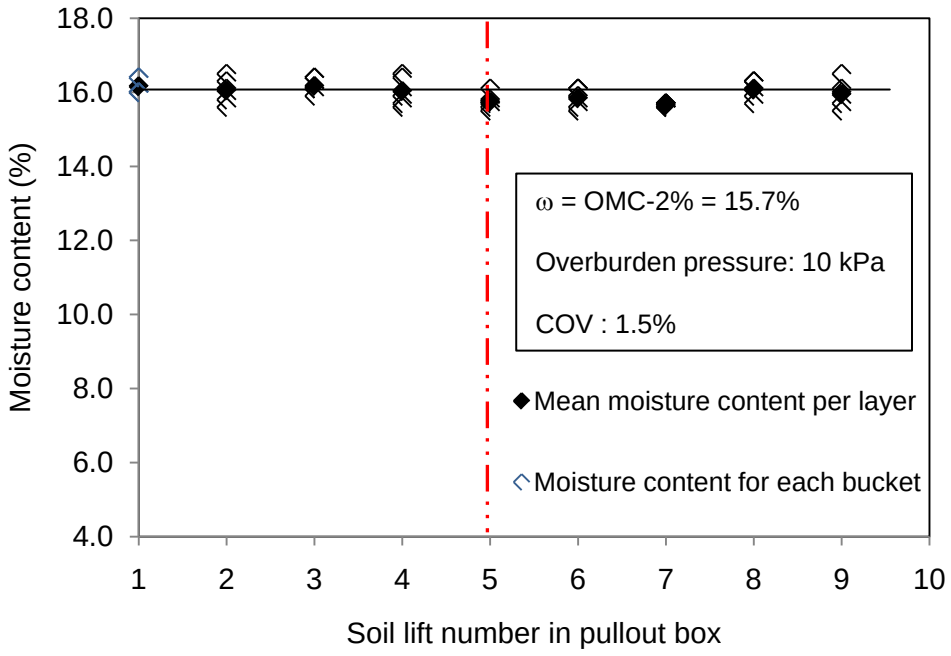


(a)

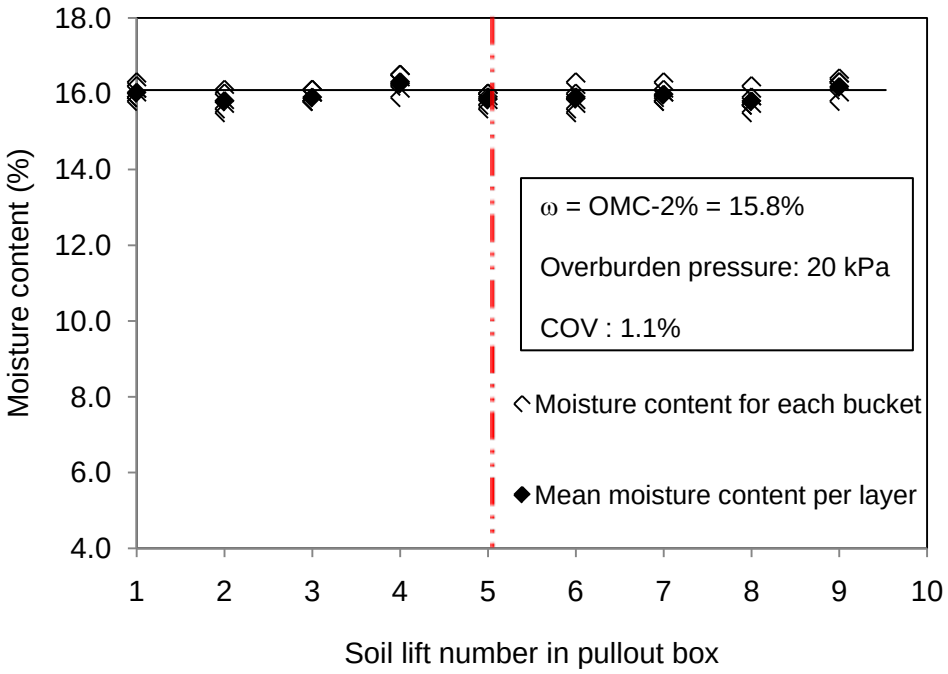
18.0
16.0
14.0
12.0
10.0
8.0
6.0
4.0
Moisture content (%)
1
2
3
4
5
6
7
8
9
10
Soil lift number in pullout box
ω = OMC-2% = 15.8%
Overburden pressure: 20 kPa
COV : 1.1%
Moisture content for each bucket
Mean moisture content per layer

(b)

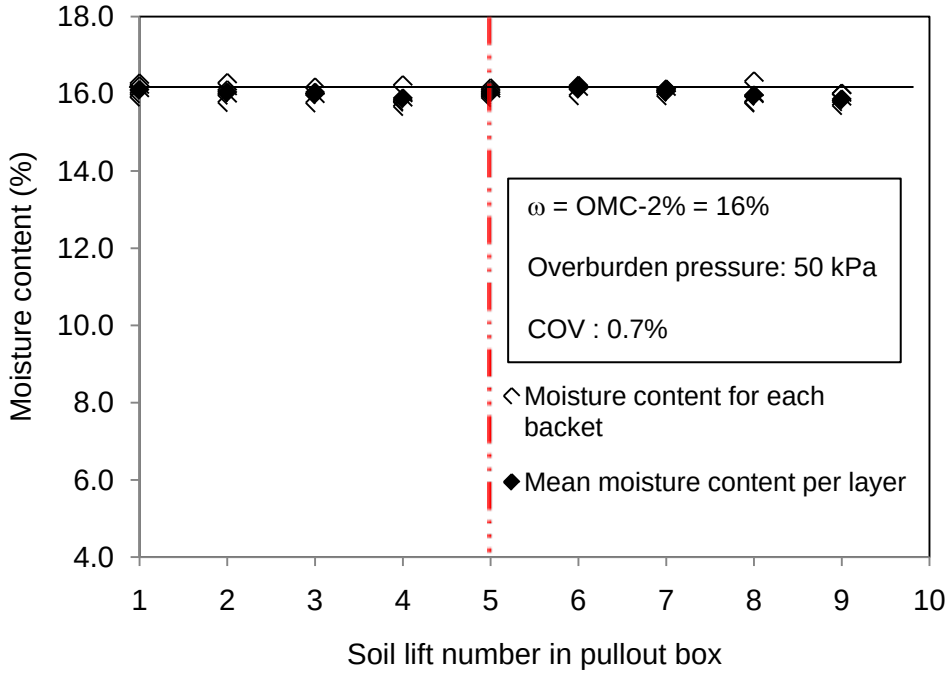
18.0
16.0
14.0
12.0
10.0
8.0
6.0
4.0
Moisture content (%)
1
2
3
4
5
6
7
8
9
10
Soil lift number in pullout box
ω = OMC-2% = 16%
Overburden pressure: 50 kPa
COV : 0.7%
Moisture content for each backet
Mean moisture content per layer

(c)

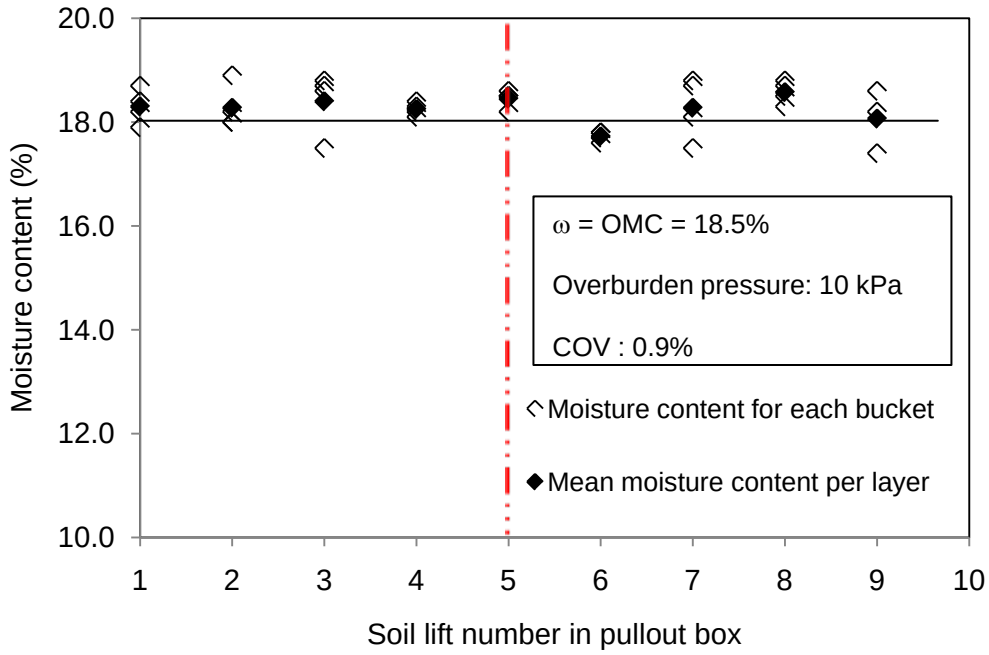
20.0
18.0
16.0
14.0
12.0
10.0
Moisture content (%)
1
2
3
4
5
6
7
8
9
10
Soil lift number in pullout box
ω = OMC = 18.5%
Overburden pressure: 10 kPa
COV : 0.9%
Moisture content for each bucket
Mean moisture content per layer

(d)

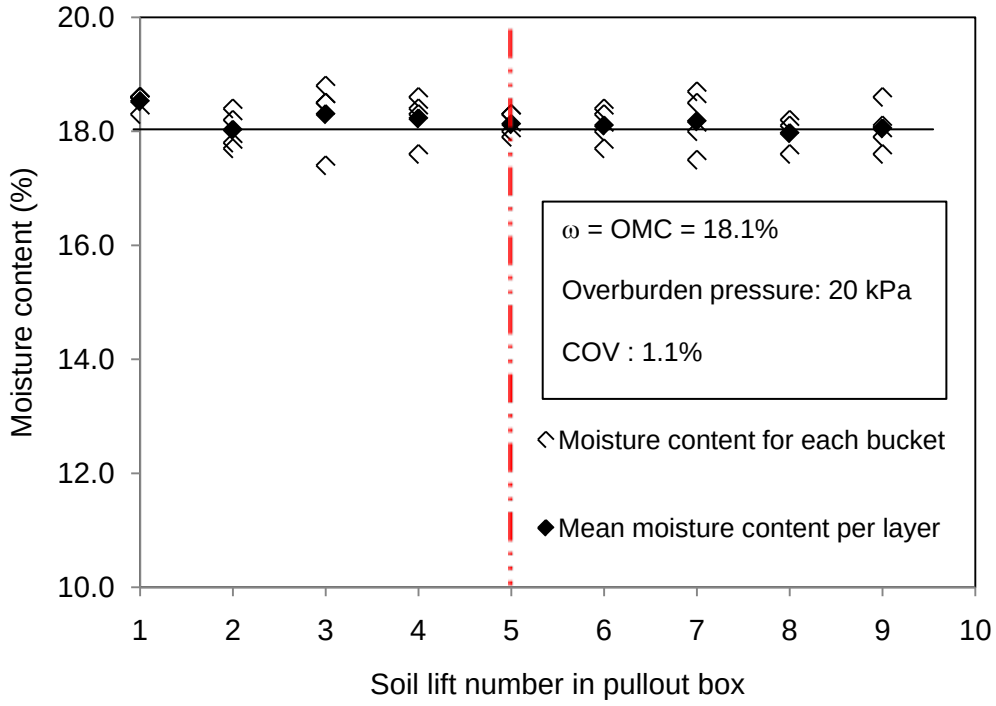
20.0
18.0
16.0
14.0
12.0
10.0
Moisture content (%)
1
2
3
4
5
6
7
8
9
10
Soil lift number in pullout box
ω = OMC = 18.1%
Overburden pressure: 20 kPa
COV : 1.1%
Moisture content for each bucket
Mean moisture content per layer

(e)

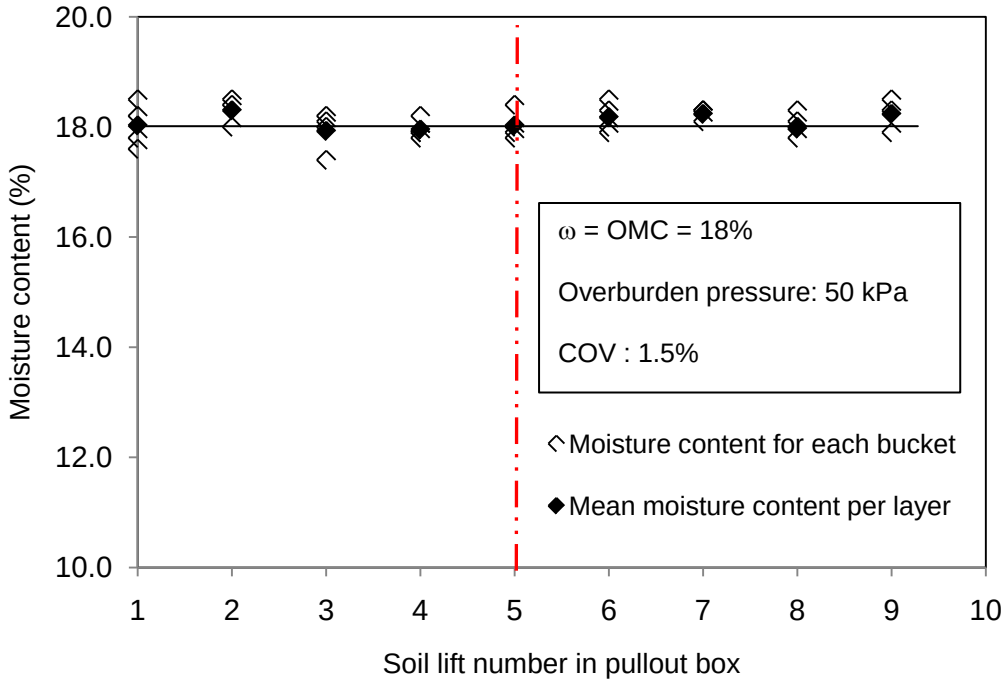
20.0
18.0
16.0
14.0
12.0
10.0
Moisture content (%)
1
2
3
4
5
6
7
8
9
10
Soil lift number in pullout box
ω = OMC = 18%
Overburden pressure: 50 kPa
COV : 1.5%
Moisture content for each bucket
Mean moisture content per layer

(f)

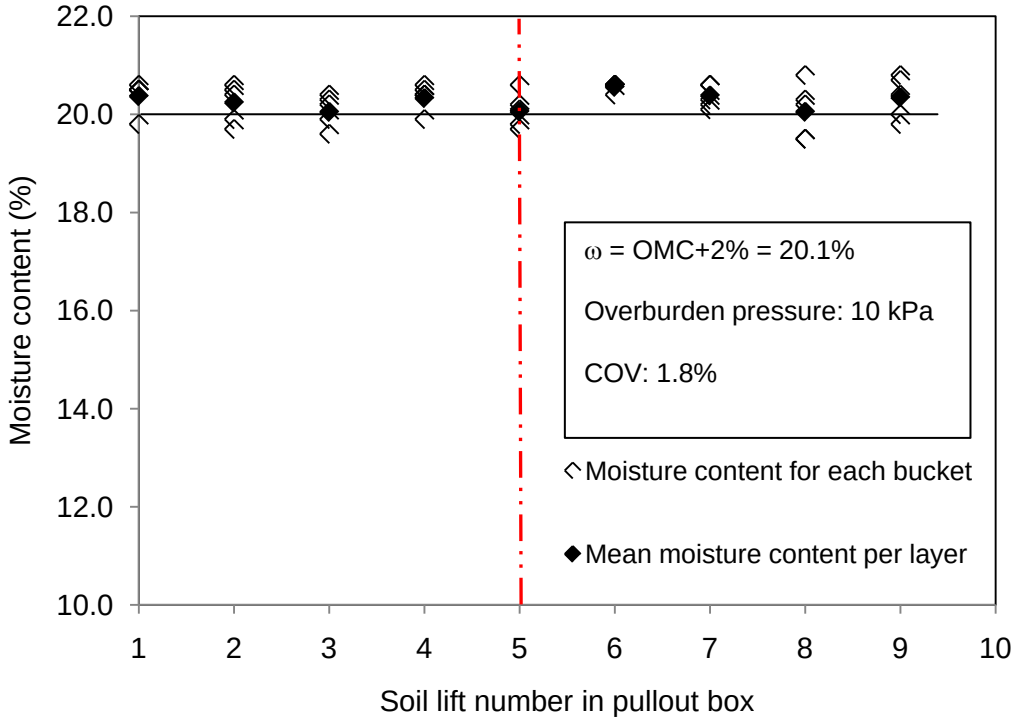
22.0
20.0
18.0
16.0
14.0
12.0
10.0
Moisture content (%)
1
2
3
4
5
6
7
8
9
10
Soil lift number in pullout box
ω = OMC+2% = 20.1%
Overburden pressure: 10 kPa
COV: 1.8%
Moisture content for each bucket
Mean moisture content per layer

(g)

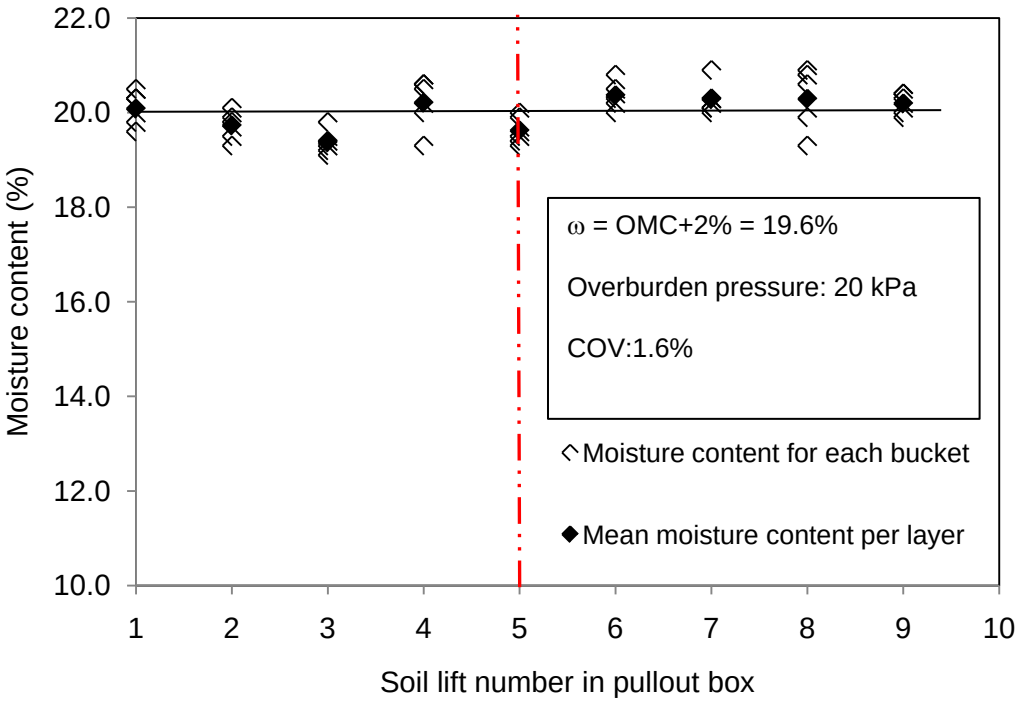


(h)

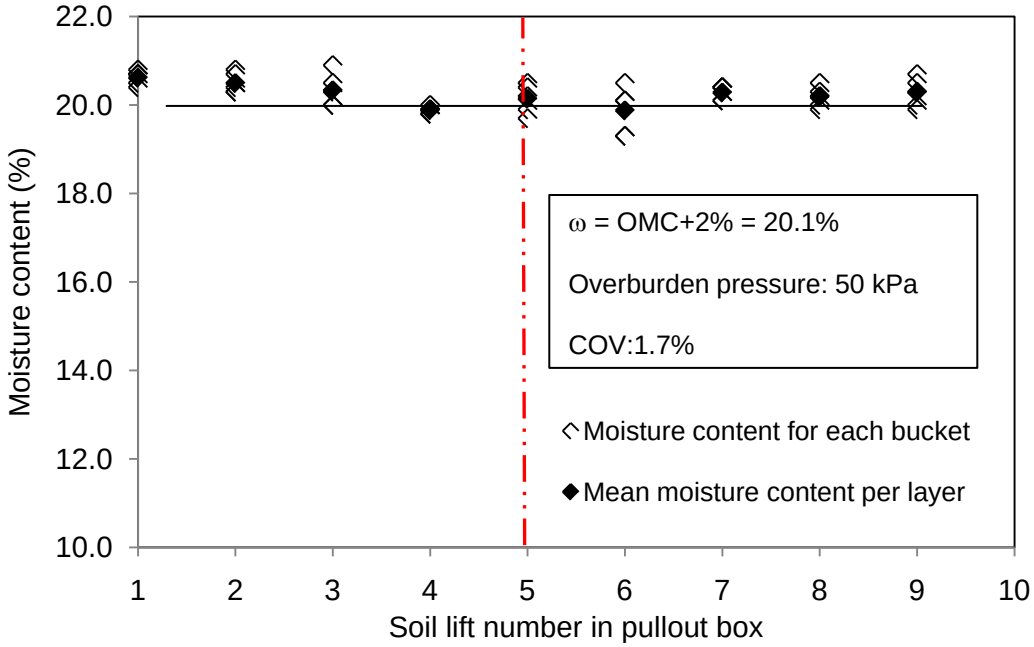


(i)

Figure 26. Distributions of moisture content over the soil depth in the pullout box. Notes: (1) One soil sample was taken from each bucket, (2) The number of soil samples from each soil lift in the pullout box is given in **Table 6** (caption), (3) the horizontal line indicates the target moisture content for each test series (4) The vertical dashed line shows the location of the soil-geotextile interfaces (5) The mean and COV values reported in the legends are calculated for the fifth layer data only.

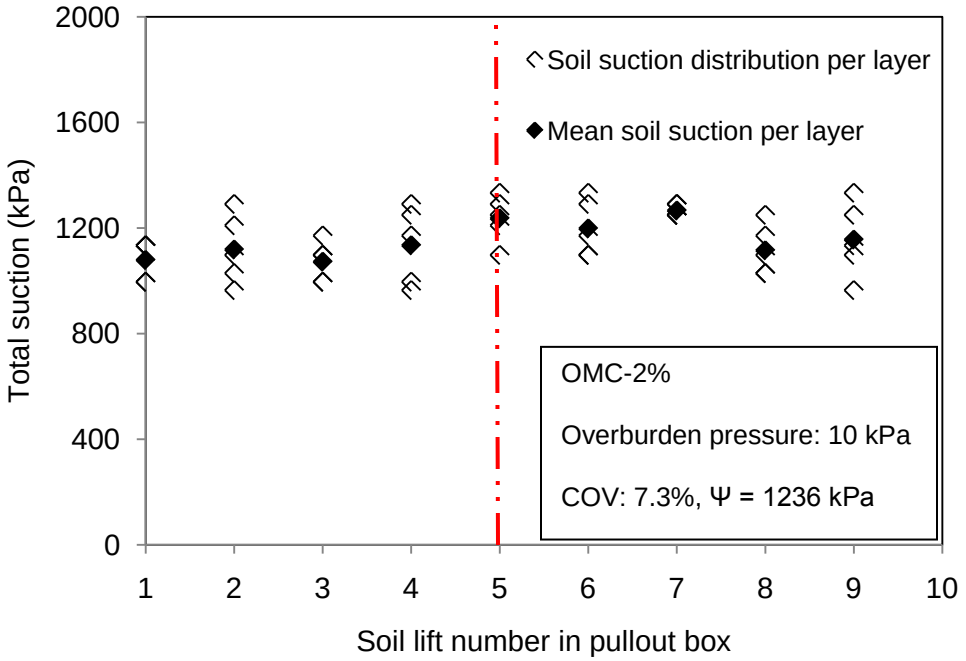
2000
1600
1200
800
400
0
Total suction (kPa)
1
2
3
4
5
6
7
8
9
10
Soil lift number in pullout box
Soil suction distribution per layer
Mean soil suction per layer
OMC-2%
Overburden pressure: 10 kPa
COV: 7.3%, Ψ = 1236 kPa

(a)

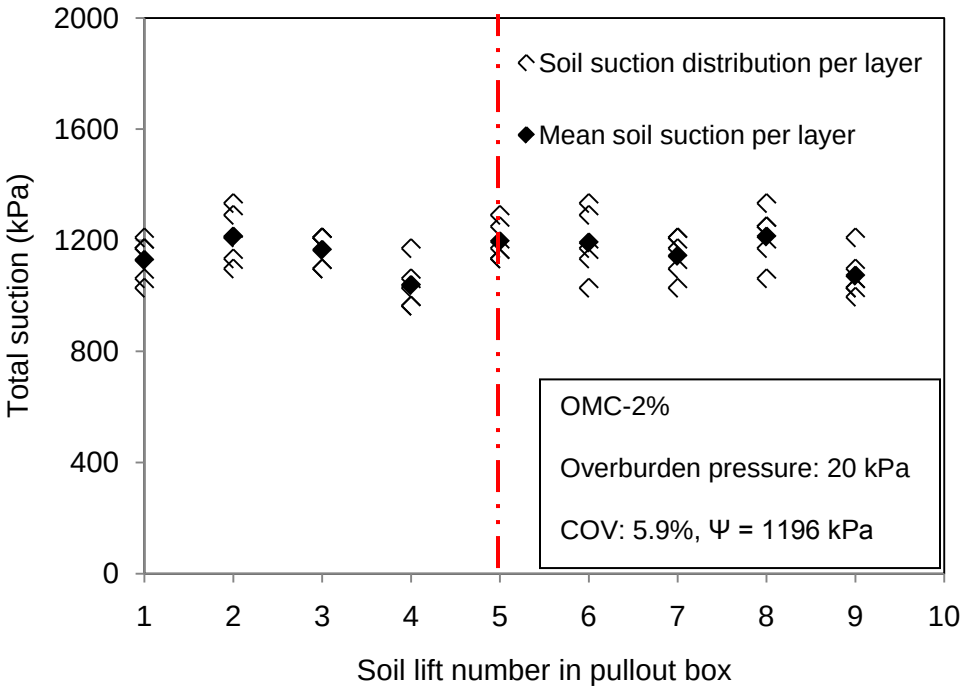
2000
1600
1200
800
400
0
Total suction (kPa)
1
2
3
4
5
6
7
8
9
10
Soil lift number in pullout box
Soil suction distribution per layer
Mean soil suction per layer
OMC-2%
Overburden pressure: 20 kPa
COV: 5.9%, Ψ = 1196 kPa

(b)

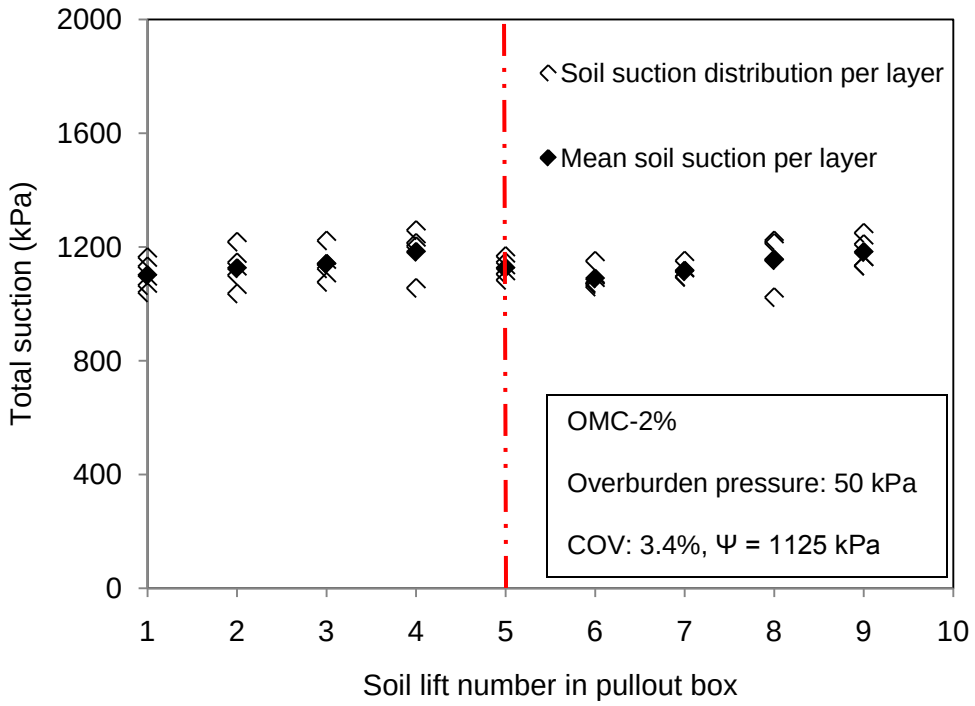
2000
1600
1200
800
400
0
Total suction (kPa)
1
2
3
4
5
6
7
8
9
10
Soil lift number in pullout box
Soil suction distribution per layer
Mean soil suction per layer
OMC-2%
Overburden pressure: 50 kPa
COV: 3.4%, Ψ = 1125 kPa

(c)

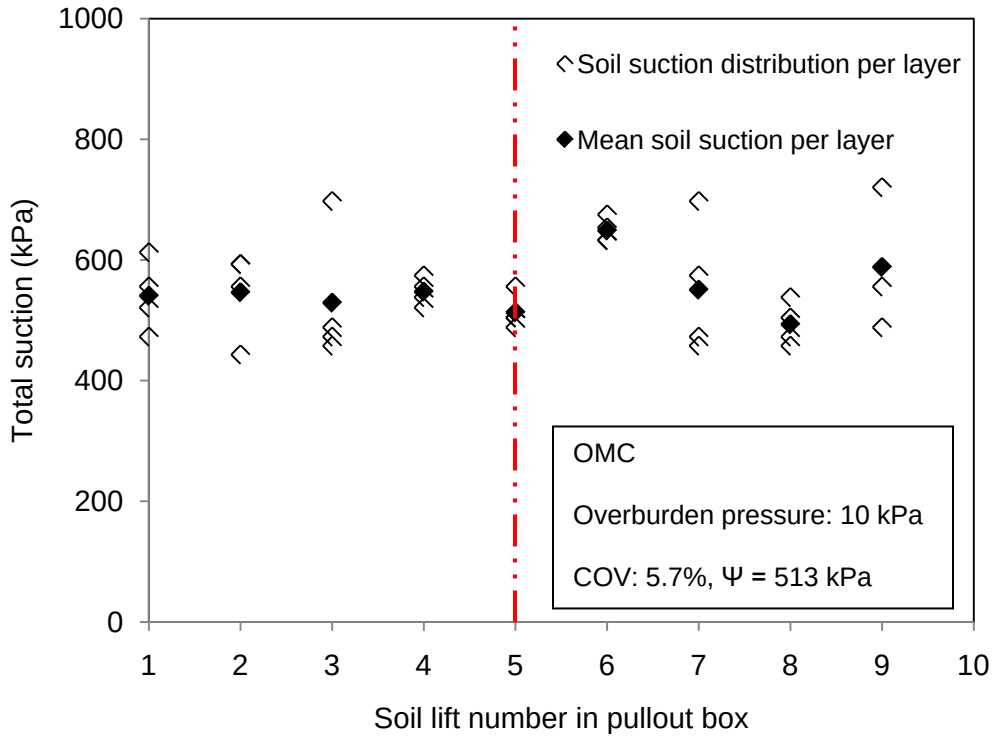
1000
800
600
400
200
0
Total suction (kPa)
1
2
3
4
5
6
7
8
9
10
Soil lift number in pullout box
Soil suction distribution per layer
Mean soil suction per layer
OMC
Overburden pressure: 10 kPa
COV: 5.7%, Ψ = 513 kPa

(d)

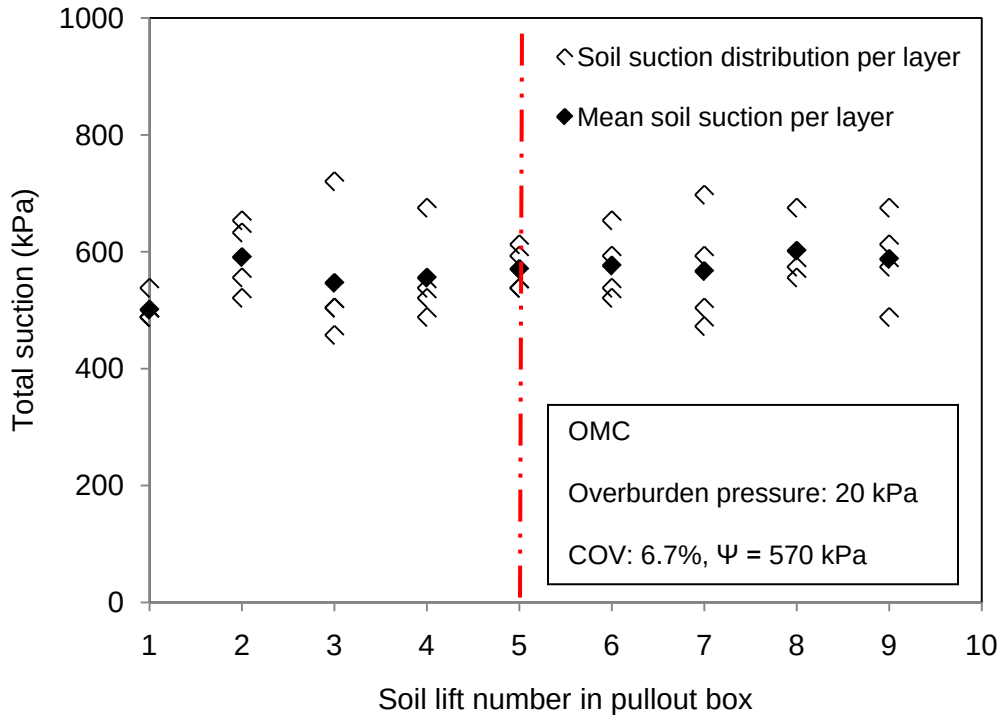
1000
800
600
400
200
0
Total suction (kPa)
1
2
3
4
5
6
7
8
9
10
Soil lift number in pullout box
Soil suction distribution per layer
Mean soil suction per layer
OMC
Overburden pressure: 20 kPa
COV: 6.7%, Ψ = 570 kPa

(e)

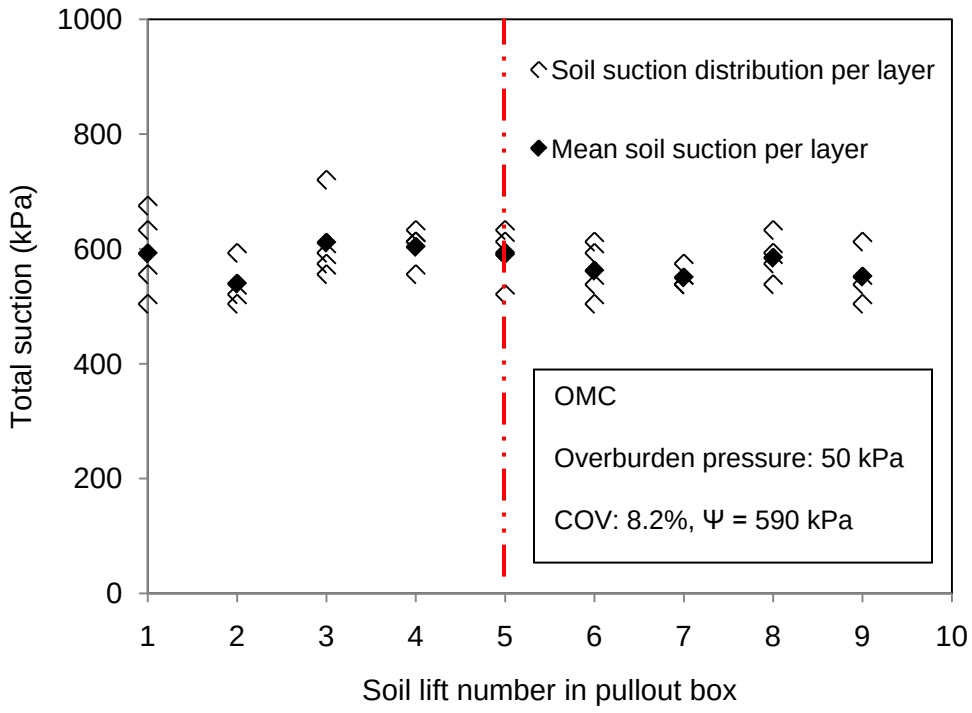
1000
800
600
400
200
0
Total suction (kPa)
1
2
3
4
5
6
7
8
9
10
Soil lift number in pullout box
Soil suction distribution per layer
Mean soil suction per layer
OMC
Overburden pressure: 50 kPa
COV: 8.2%, Ψ = 590 kPa

(f)

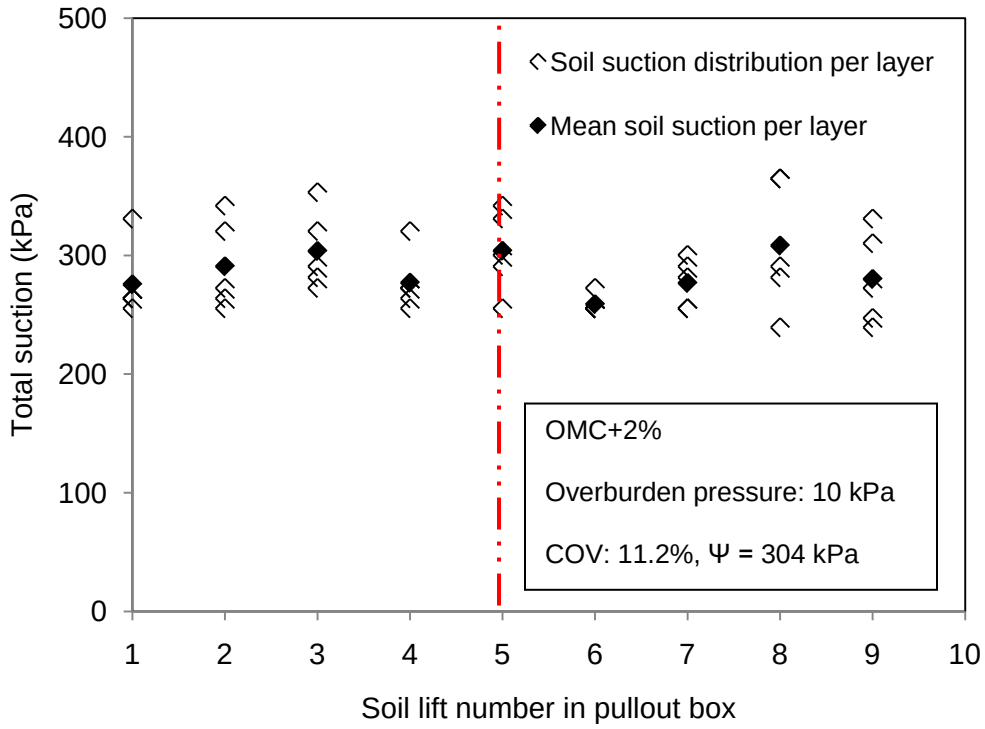
Soil suction distribution per layer
Mean soil suction per layer
OMC+2%
Overburden pressure: 10 kPa
COV: 11.2%, Ψ = 304 kPa
Total suction (kPa)
Soil lift number in pullout box
0
100
200
300
400
500
1
2
3
4
5
6
7
8
9
10

(g)

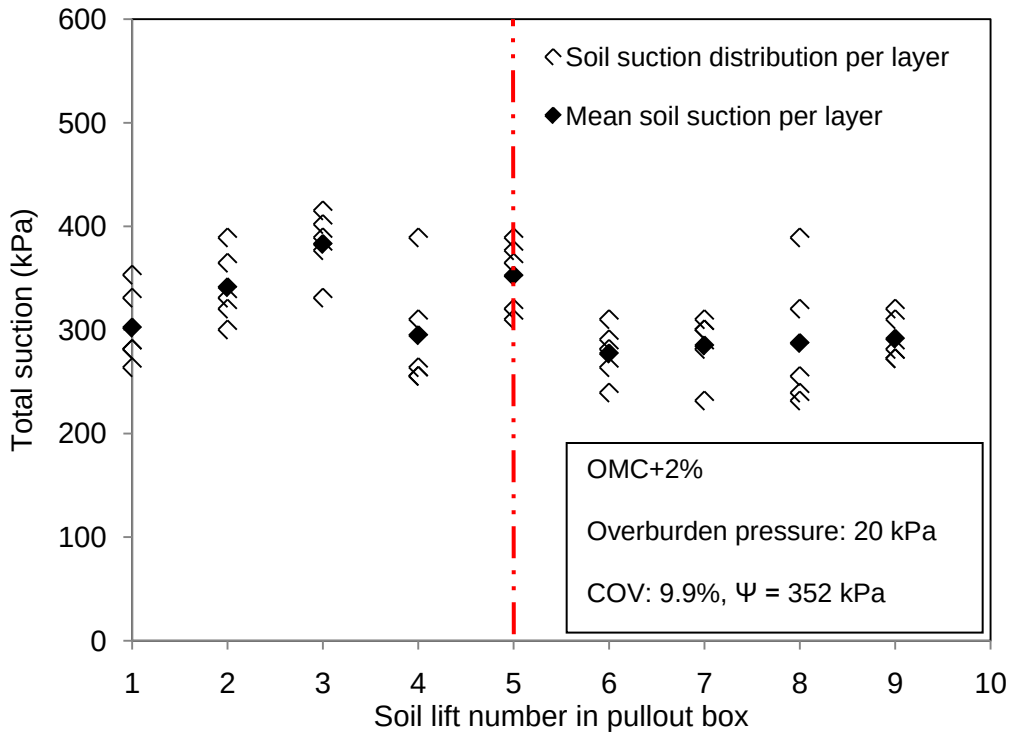
Soil suction distribution per layer
Mean soil suction per layer
OMC+2%
Overburden pressure: 20 kPa
COV: 9.9%, Ψ = 352 kPa
Total suction (kPa)
Soil lift number in pullout box
0
100
200
300
400
500
600
1
2
3
4
5
6
7
8
9
10

(h)

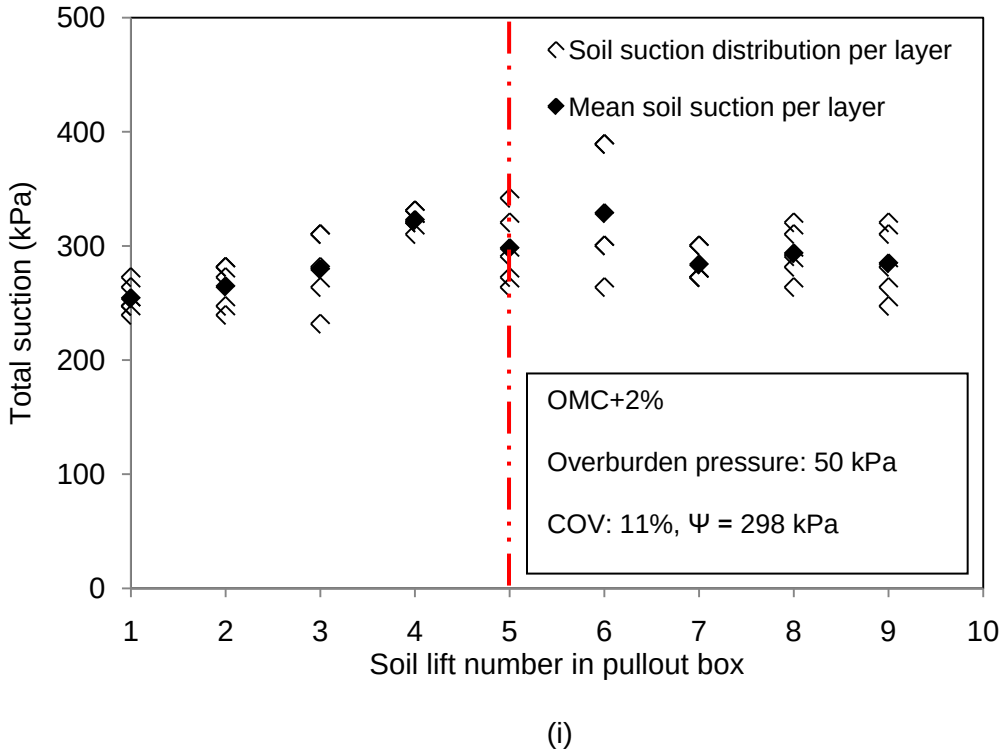


(i)

Figure 27. Distributions of total suction over the soil depth in the pullout box from WP4 at different moisture contents. Note: the number of soil samples from each soil lift in the pullout box is given in **Table 6** (caption).

**Figure 28** shows the pullout test data for Chickasha soil at different overburden pressure, suction and moisture content values. The measured pullout force is plotted as a function of the actuator displacement. The interface strength results for the geotextile reinforcement in Chickasha soil are also shown in **Figure 28** and summarized in **Table 9.** The interface strength values in **Table 9** correspond to the maximum pullout resistance values shown in **Figure 28**.

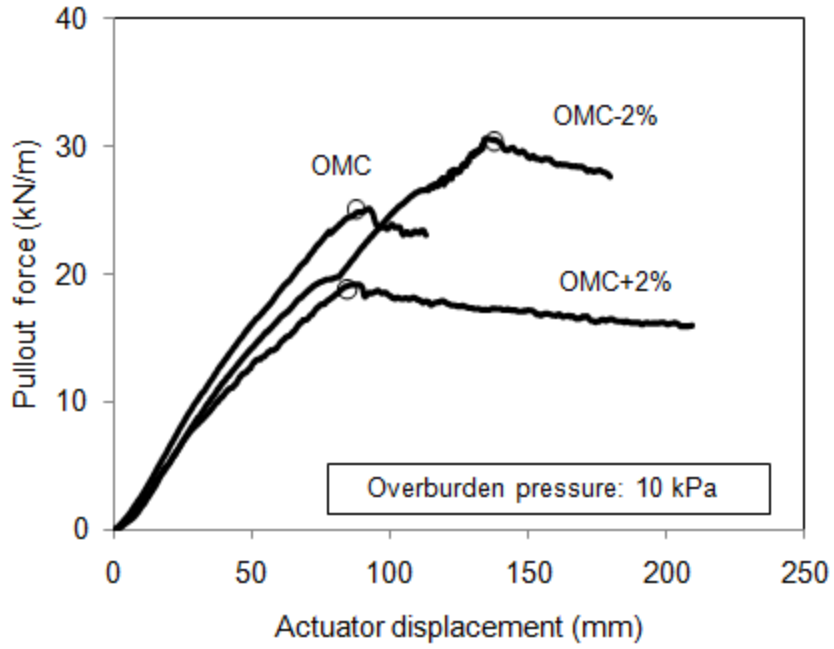
40
30
20
10
0
Pullout force (kN/m)
OMC-2%
OMC
OMC+2%
Overburden pressure: 10 kPa
0
50
100
150
200
250
Actuator displacement (mm)

(a)

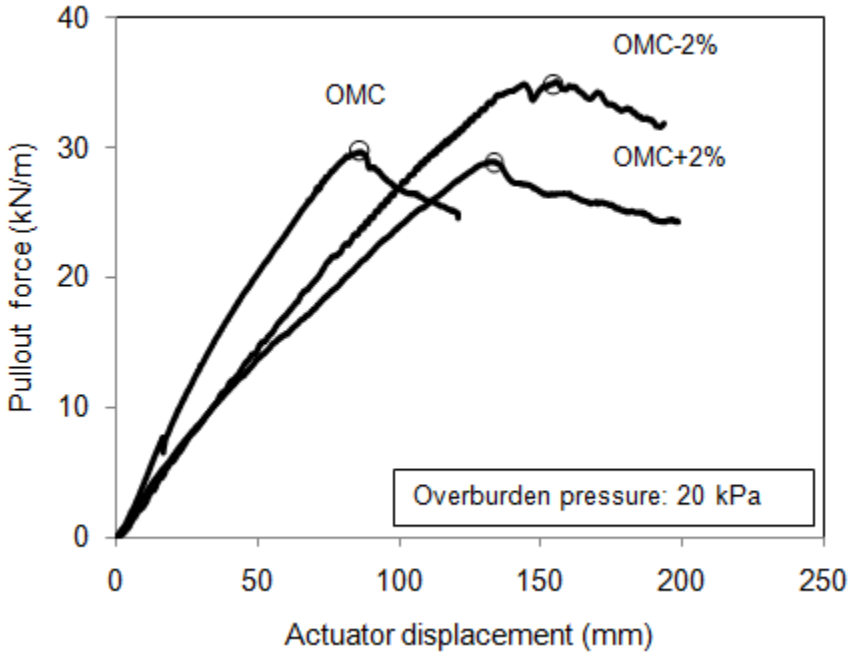
40
30
20
10
0
Pullout force (kN/m)
OMC-2%
OMC
OMC+2%
Overburden pressure: 20 kPa
0
50
100
150
200
250
Actuator displacement (mm)

(b)

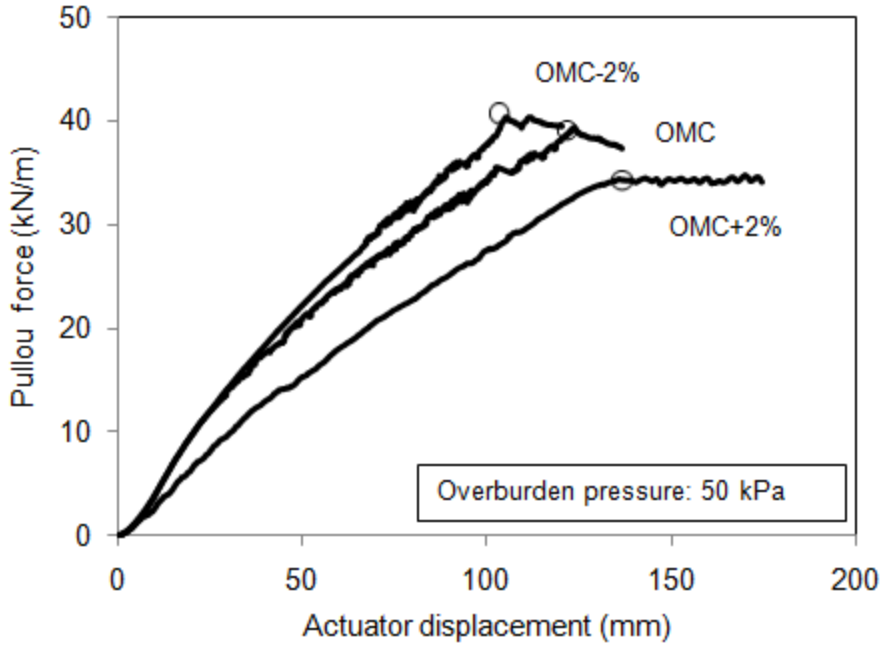


(c)

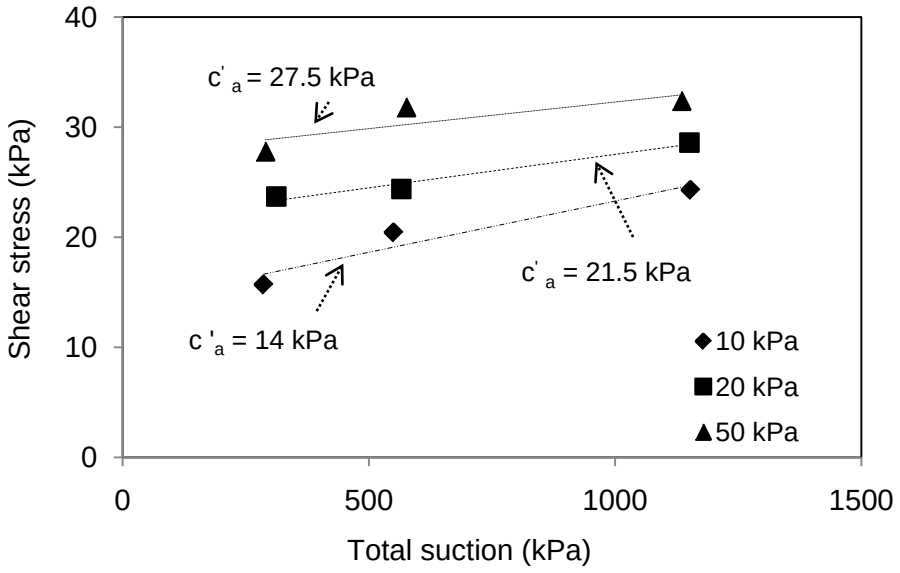


(d)

Figure 28. Pullout test data and interface strength results for Chickasha soil at different overburden pressure values and comparison of failure envelopes for soil-geotextile interface on lateral plane at different moisture contents (OMC-2%, OMC, OMC+2%).

Table 9. Interface strength properties from pullout tests in Chickasha soil as a function of the soil total suction

| $\sigma_n$ (kPa) (psf) | Average ω (%) | Average Ψ (kPa) | $P_r$ (kN/m) | $\tau_{max}$ (kPa) | $c'_a$ (kPa) |
|---|---|---|---|---|---|
| 10 (208) | 16 | 1153 | 29.6 | 24.3 | 27.5 |
| | 18.3 | 550 | 24.8 | 20.4 | |
| | 20.3 | 286 | 19.1 | 15.7 | |
| 20 (417.7) | 16 | 1151 | 34.8 | 28.6 | 21.5 |
| | 18.2 | 566 | 29.7 | 24.4 | |
| | 20 | 312 | 28.8 | 23.7 | |
| 50 (1044.3) | 16 | 1135 | 39.4 | 32.4 | 14 |
| | 18.1 | 576 | 38.7 | 31.8 | |
| | 20.2 | 290 | 33.8 | 27.8 | |

Results in **Figure 28** show the failure envelopes of the three-dimensional extended Mohr-Coulomb failure surfaces on the lateral plane for the soil-geotextile interface as a function of suction. The line intercept and slope represent the effective adhesion at zero overburden pressure ($\sigma_n = 0$ kPa) and interface friction angle with respect to suction ($\delta^b$), respectively. The data shown in **Figure 28d** indicate that the interface friction angle with respect to suction for the Chickasha soil-geotextile tested is negligible (i.e. it is less than 1°; note the significantly different scales of the horizontal and vertical axes in the figure).

**Figure 29** summarizes the frontal and lateral failure envelopes of the extended Mohr-Coulomb surfaces for the soil-geotextile interaction at different overburden pressure ($\sigma_n$) and suction ($\Psi$) values.

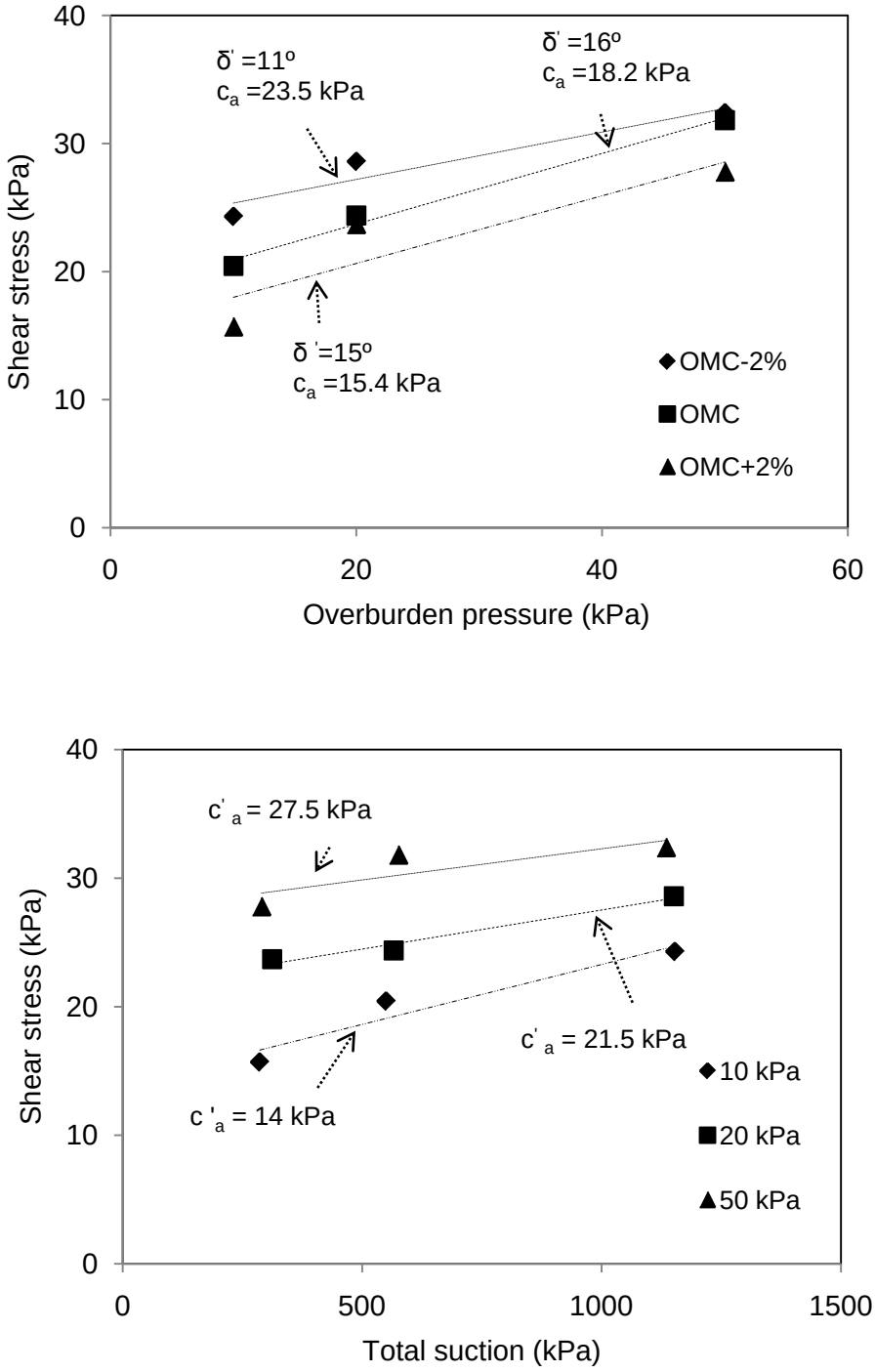


Figure 29. Extended Mohr-Coulomb failure envelopes for the soil-geotextile interface from large-scale pullout tests

### 4.2.6. PARAMETERS $\alpha$ AND $F^*$

Large-scale pullout tests in Chickasha soil were used to obtain pullout parameters for the geotextile reinforcement including the values for α and $F^*$ (Berg et al. 2009) in **Equation 1**. The correction factor ($\alpha$) represents the reinforcement extensibility. The parameter $F^* = \tan \delta_{peak}$, in general, includes the contributions of both passive and frictional resistance components in the reinforcement pullout resistance. **Table 10** shows $\alpha$ and $F^*$ values for all large scale pullout tests carried out in this study. Example calculations according to the FHWA (Berg et. al. 2009) recommended method to determinate $\alpha$ are shown in **Figure 30**. First, the measured pullout force was plotted as a function of the actuator displacement. Second, the normalized pullout displacement was plotted versus mobilized reinforcement length ($L_p$). Different mobilized lengths were obtained from four wire extensometers attached to the geotextile reinforcement surface. Third, the value of $P_r$ for each confining pressure magnitude ($\sigma_v$) was plotted versus $\sigma_v L_p$ from which the values for $F_{peak}$ and $F_m$ were determined. Finally, the correction factor ($\alpha$) was plotted versus $L_p$. A hyperbolic curve was fitted to the data shown in (**Figure 30e**) to determine the scale effect correction factor ($\alpha$). A software called Graphsite (Cradle fields company 2004) was used to plot the hyperbolic regression through the data points. The choice of a hyperbolic curve with a horizontal asymptote is consistent with the objective in the FHWA procedure to determine the value of $\alpha$ for the reinforcement at field scale. Based on the intersection of the horizontal asymptote with the y-axis, the design value for $\alpha$ from our pullout tests in Chickasha soil was found to be 0.53 (**Figure 30e**). This value of $\alpha$ is comparable to that reported by Hatami et al. (2010a) for the same geotextile material tested in Minco silt (i.e. $\alpha$ = 0.59) and is close to the value $\alpha$ = 0.6 as recommended by FHWA (Berg et. a. 2009) for geotextiles. **Figure 31** shows the variation of $P_r$ (pullout resistance) versus $L_p$ (mobilized length). Results in **Figure 31** indicate that for a given value of pullout resistance, the mobilized reinforcement length is smaller for a greater overburden pressure.

Table 10. Large-scale pullout tests in Chickasha soil to obtain values for $\alpha$ and $F^*$

| Target ω (%) | $\sigma_n$ (kPa) | $P_r$ (kN/m) | $\tau_{peak}$ (kPa) | $\alpha$ | $F^* = \tau_{peak}/\sigma_n$ |
|---|---|---|---|---|---|
| 16 % (OMC-2%) | 10 | 29.6 | 24.3 | 0.52 | 2.43 |
| | 20 | 34.8 | 28.6 | 0.53 | 1.43 |
| | 50 | 39.4 | 32.4 | 0.52 | 0.65 |
| 18 % (OMC) | 10 | 24.8 | 20.4 | 0.50 | 2.04 |
| | 20 | 29.7 | 24.4 | 0.53 | 1.22 |
| | 50 | 38.7 | 31.8 | 0.50 | 0.64 |
| 20 % (OMC+2%) | 10 | 19.1 | 15.7 | 0.54 | 1.57 |
| | 20 | 28.8 | 23.7 | 0.53 | 1.19 |
| | 50 | 33.8 | 27.8 | 0.50 | 0.56 |

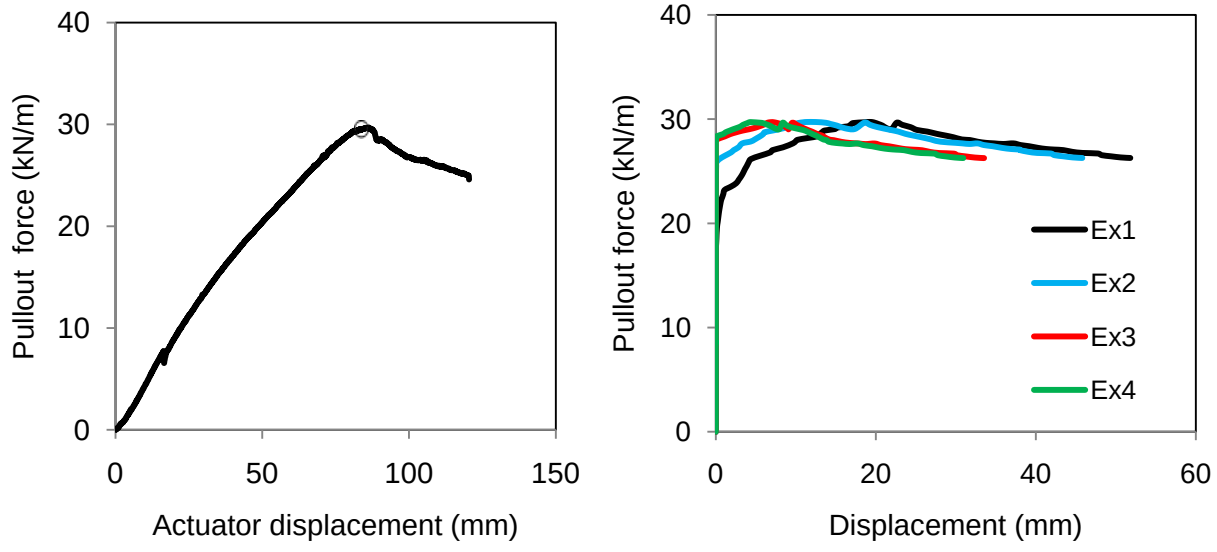


(a) (b)

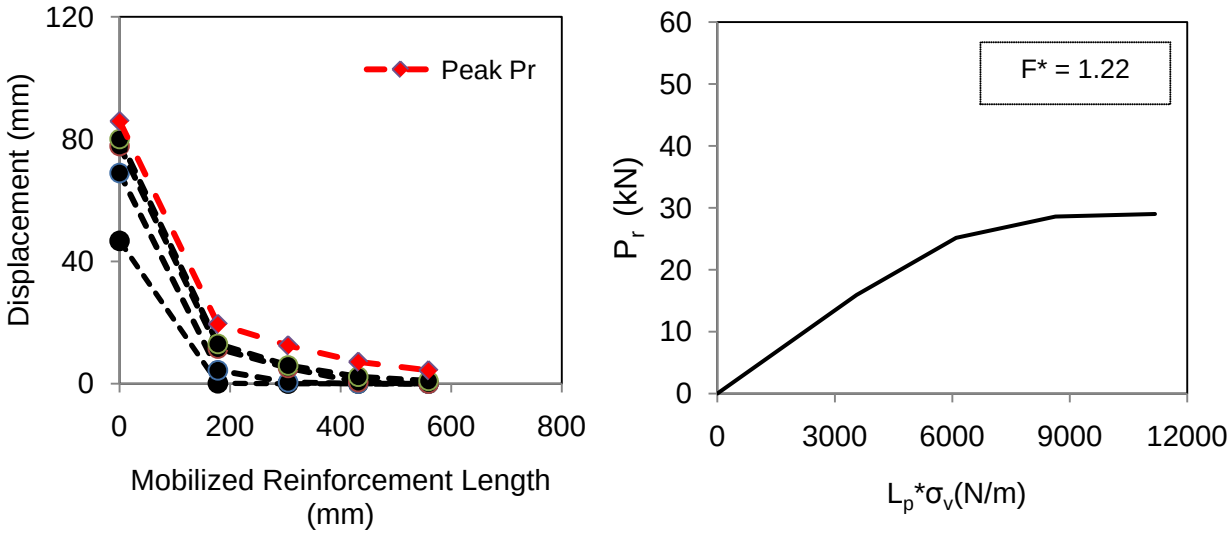


(c) (d)

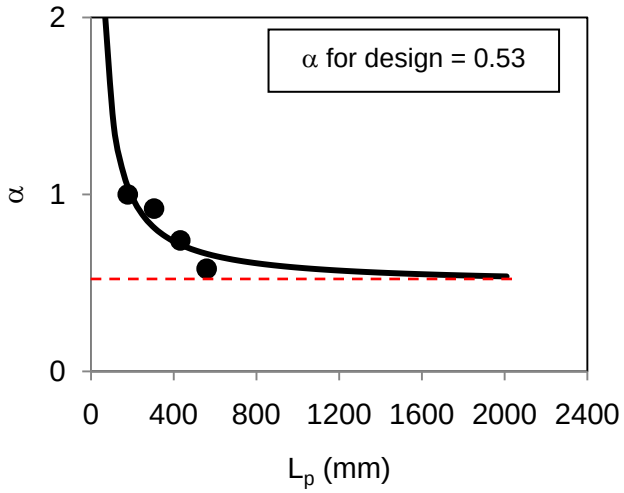


(e)

Figure 30. Calculation of pullout parameters for Mirafi HP370 geotextile reinforcement from large-scale pullout test data in Chickasha soil.

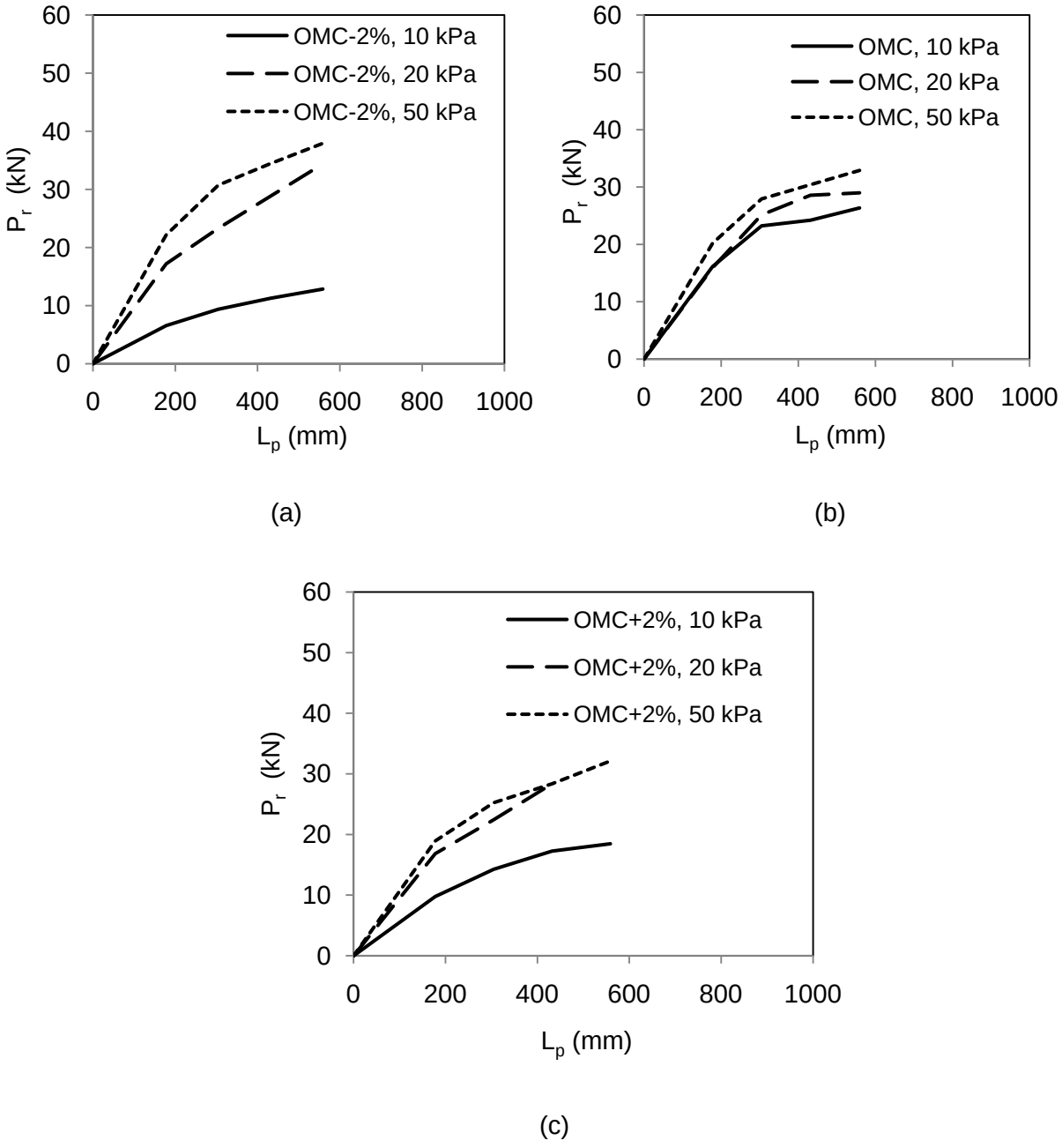


Figure 31. Pullout resistance versus mobilized length at different overburden pressure values.

## 5. SMALL-SCALE TESTS

In addition to large-scale pullout tests, a series of small-scale pullout tests and interface shear tests were performed to develop a better understanding of the influence of soil moisture content on marginal soil-geotextile interfaces using a multi-scale laboratory testing approach. The small-scale tests were carried out on the same soil used in the large-scale pullout tests. In addition, these tests were carried out at the same soil moisture contents (OMC-2%, OMC and OMC+2%), unit weight (i.e. 95% of maximum dry unit weight from standard Proctor test) and overburden pressure magnitudes (10 kPa, 20 kPa and 50 kPa) as those in the large-scale pullout tests (**Table 11**).

Table 11. Small-scale pullout test parameters

| Test information | Chickasha Soil |
|---|---|
| Type of small-scale test | Pullout, Interface shear |
| Geosynthetic reinforcement | Mirafi HP370, woven PP |
| Overburden pressure, kPa (psf) | 10 (208), 20 (417.7), 50 (1044.3) |
| Moisture content | OMC-2%, OMC, OMC+2% |

Pullout tests and interface shear tests were carried out using the direct shear testing (DST) equipment at the OU Geotechnical Testing Laboratory. The soil in both tests was placed in a 59.7 mm × 59.7 mm (2.35" × 2.35") square test cell that was supplied with the test equipment. A rectangular block of Styrofoam with dimensions 60 mm (W), 23 mm (H) and 9 mm (T) was used in the small-scale pullout tests in front of the soil specimen to provide a compressible boundary condition similar to that in the large-scale pullout box. A 0.8" (W) × 1.6" (L) geotextile specimen was used in each pullout test. The linear scale factor between the small-scale and large-scale pullout tests was 1:15. In the pullout tests, the geotextile specimen was pulled out of a fixed test cell filled with Chickasha clay at a speed of 0.06 mm/min (i.e. 1/15 of 1 mm/min nominal rate at large scale). In the direct shear tests, the lower box of the DST machine was pushed laterally at a speed of 0.06 mm/min to apply a shear load on the soil-geotextile interface.

## 5.1. SMALL-SCALE PULLOUT TESTS

Pullout tests were carried out in Chickasha soil at OMC-2%, OMC and OMC+2% (**Figure 32**). Clay was prepared for small-scale pullout tests using the same process as was followed for the large-scale tests: The clay was first processed, then passed through #4 sieve in a 7-tray Gilson screen shaker and mixed with water to reach the target moisture content and its moisture content was measured using the oven drying method preceding and following each test. The bottom half of the 59.7 mm × 59.7 mm (2.35" × 2.35") test cell was filled with four layers of Chickasha soil at target moisture content and each layer was compacted to 3 mm (0.12 in). The geotextile specimen was attached to a custom-made clamp mounted on the test box and was embedded 40.7 mm (1.6 in) inside the test cell. A U-shape metal spacer was used to maintain a gap within the pullout slot to prevent any frictional contacts within the test cell frame during the pullout process. The top half of the box was filled with 4 more layers of clay, each compacted to 3 mm (0.12 in) thickness.

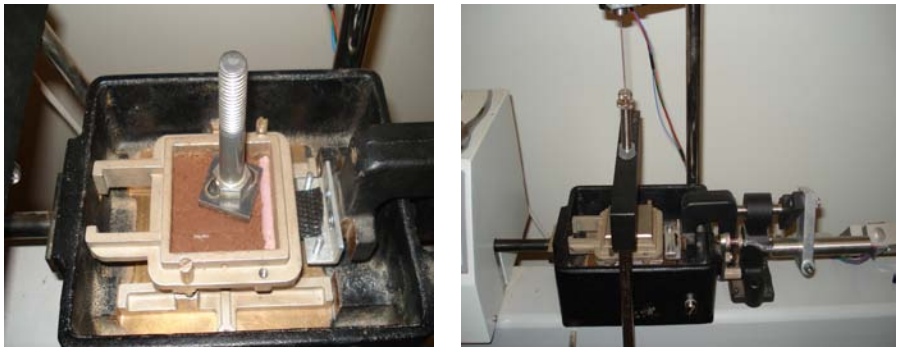

Figure 32. Small-scale pullout tests in Chickasha soil using a DST machine

### 5.1.1. RESULTS

**Figure 33** shows the plots of mean interface shear stress versus displacement for pullout tests in Chickasha soil at OMC-2%, OMC and OMC+2%. The mean interface shear stress values were calculated by dividing the pullout force by the soil-geotextile interface area for each test case. It is observed that the shear stress increases with the overburden pressure. Soil-geotextile interface strength properties obtained from the small-scale tests are summarized in **Table 12**.

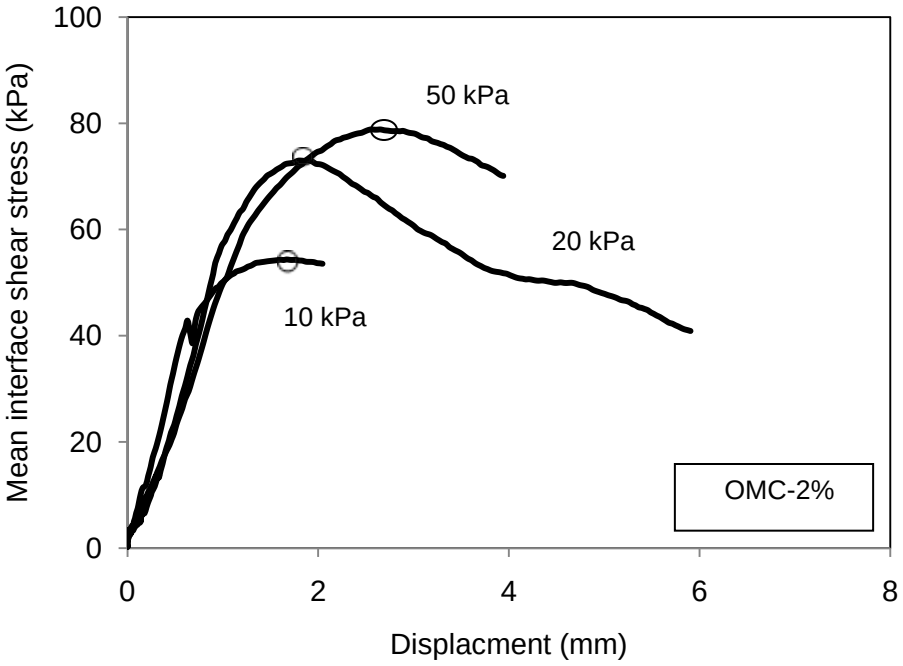
100
80
60
40
20
0
Mean interface shear stress (kPa)
50 kPa
20 kPa
10 kPa
OMC-2%
0
2
4
6
8
Displacment (mm)

(a)

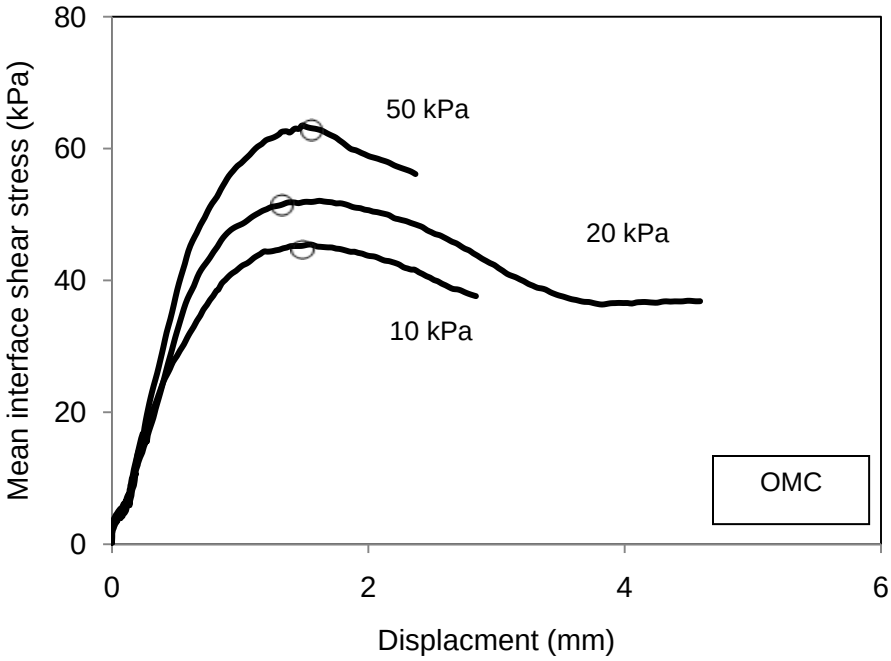
80
60
40
20
0
Mean interface shear stress (kPa)
50 kPa
20 kPa
10 kPa
OMC
0
2
4
6
Displacment (mm)

(b)

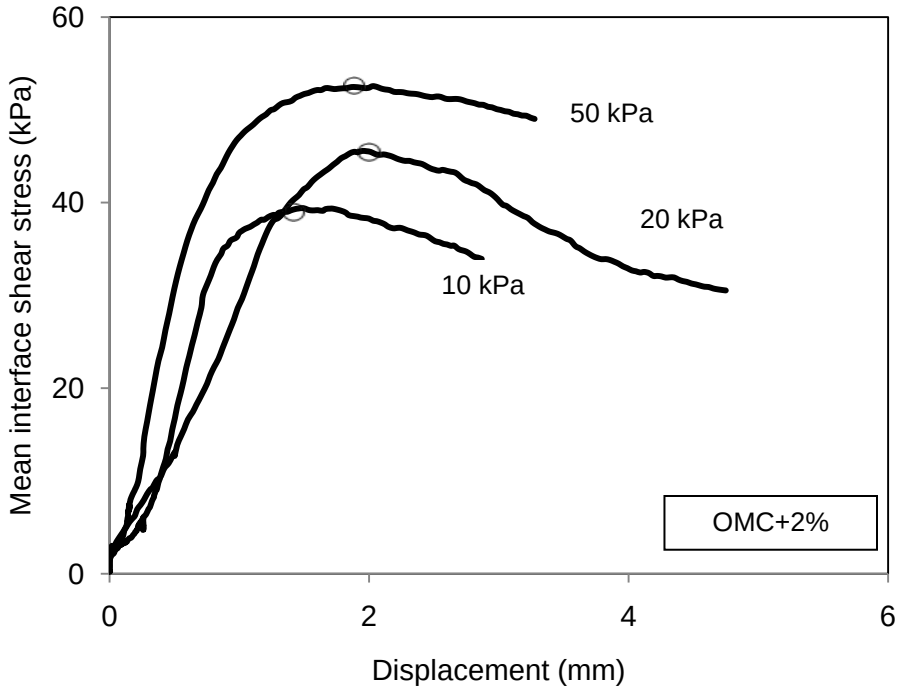


(c)

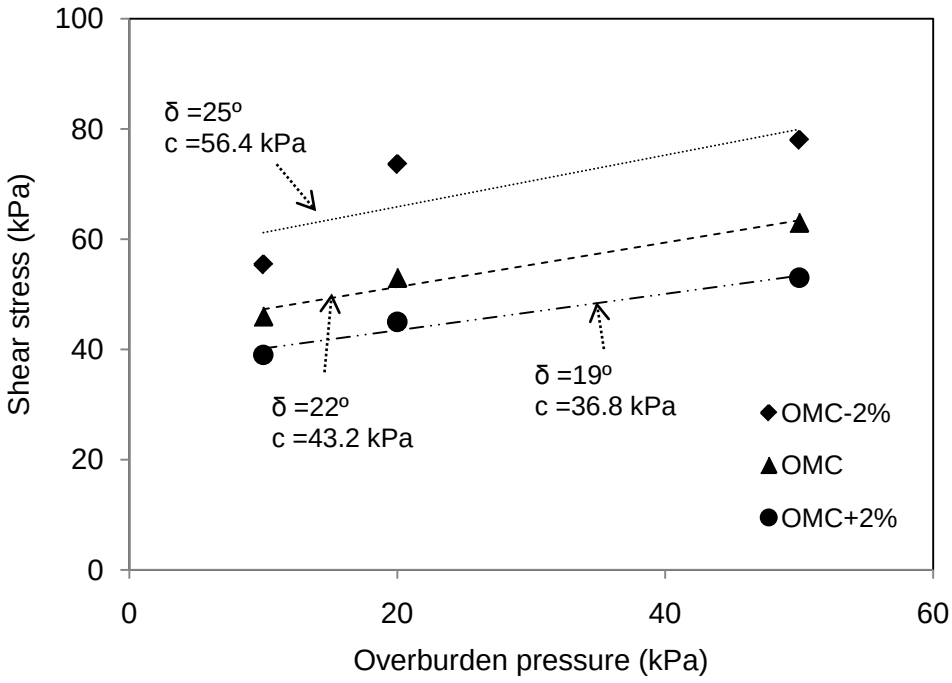


(d)

Figure 33. Pullout test data and interface strength results for Chickasha soil and comparison of failure envelopes for soil-geotextile interface at different moisture contents (OMC-2%, OMC, OMC+2%).

Table 12. Interface strength properties from small-scale pullout tests

| Target ω (%) | $\sigma_n$ (kPa) (psf) | ω (%) | Ψ (kPa) | $\tau_{max}$ (kPa) | $\delta'$ (º) | $C_a$ (kPa) |
|---|---|---|---|---|---|---|
| 16(OMC-2%) | 10 (208) | 16.3 | 1036 | 55.4 | 25 | 56.4 |
| | 20 (417.7) | 15.9 | 1164 | 73.6 | | |
| | 50 (1044.3) | 16 | 1131 | 78.5 | | |
| 18 (OMC) | 10 (208) | 17.8 | 633 | 45.9 | 22 | 43.2 |
| | 20 (417.7) | 17.9 | 613 | 52.8 | | |
| | 50 (1044.3) | 18.3 | 538 | 62.9 | | |
| 20 (OMC+2%) | 10 (208) | 20 | 310 | 39.2 | 19 | 36.8 |
| | 20 (417.7) | 19.9 | 320 | 44.8 | | |
| | 50 (1044.3) | 19.8 | 331 | 53.1 | | |

The pullout test results shown in **Table 12** and **Figure 33** show a clear influence of the soil moisture content on the clay-geotextile interface strength and pullout resistance. The interface adhesion contributing to the geotextile pullout resistance decreases as the soil moisture content increases from OMC-2% to OMC+2%. However, the change in the interface strength is significant on the dry side of optimum. In other words, the reduction in the interface strength is more pronounced between OMC-2% to OMC as compared to the difference between the strength values at OMC and OMC+2%. On the other hand, changes in the interface friction angle are practically negligible. These results are consistent with those obtained by the authors in a previous study on Minco silt (Hatami et al. 2010a,b). This observation can be explained by the fact that the soil water characteristic curves (SWCC) of these soils are concave upward. This means that the drop in suction from OMC-2% to OMC is greater than its decrease between OMC and OMC+2%. Therefore, the interface strength is more significantly influenced by the soil suction on the dry side of the OMC than on the wet side of optimum.

**Figure 34** shows the graphs of maximum shearing stress versus overburden pressure for both large-scale and small-scale pullout tests in Chickasha soil at different moisture content values. Results in **Figure 34** show that the effective adhesion from both small-scale and large-scale

pullout tests is consistently higher for greater soil suction values (i.e. lower soil moisture content). This indicates that the effective adhesion depends on the soil moisture content.

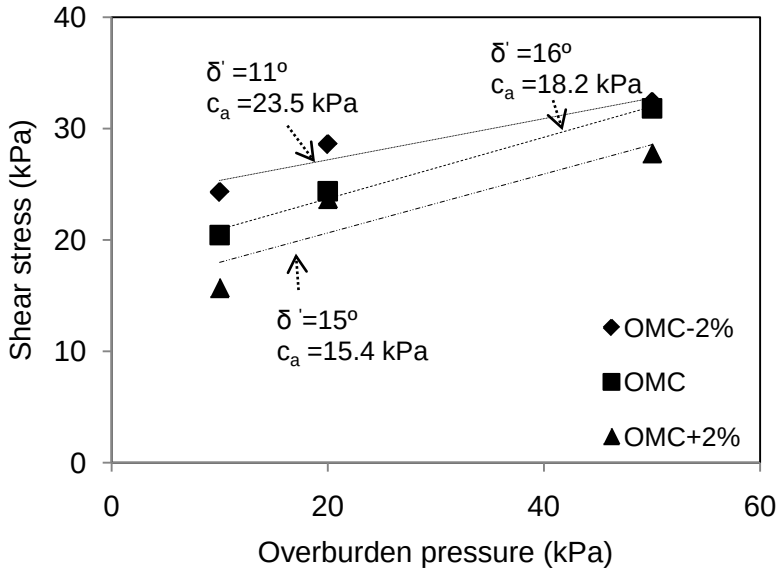


(a)

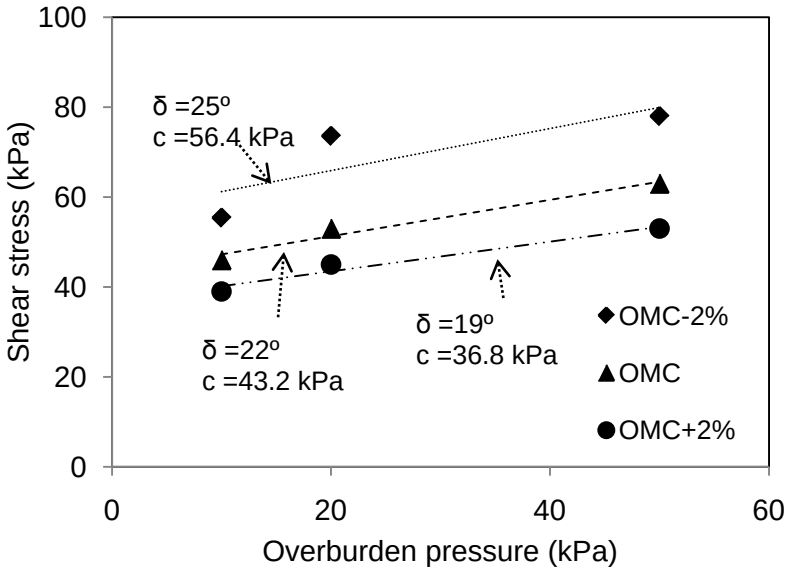


(b)

Figure 34. Chickasha soil-geotextile interface strength results from pullout tests: (a) Large-scale-scale tests, (b) Small-scale tests

Results shown in **Figure 34** also indicate that the soil-geotextile interface strength properties from small-scale pullout tests are greater than those from the corresponding large-scale tests. This could be attributed to smaller size and greater boundary effects in the small-scale tests. The next phase of this study will include determining a calibration factor that could be used to predict large-scale pullout test results based on those of small-scale tests on the same materials.

## 5.2. INTERFACE SHEAR TESTS

A series of interface shear tests was carried out on the HP370 woven geotextile with Chickasha soil at different moisture content values to determine the Chickasha soil-geotextile interface properties (interface adhesion and friction angle). Filler aluminum panels were placed in the bottom half of the test cell in the DST machine. A geotextile specimen was attached to an aluminum panel and placed on the top in the bottom half of the test cell. The top half of the test cell was filled with four layers of Chickasha soil each of which was 3 mm (0.12 in) thick after compaction.

### 5.2.1. RESULTS

**Figure 35** shows the Mohr-Coulomb envelopes from interface shear tests at OMC-2%, OMC and OMC+2% moisture content values. As expected, interface adhesion increases with both the overburden pressure and the soil suction resulting in an increase in the soil-geotextile interface strength. The interface friction angle was found to be practically independent of the soil suction. These results are consistent with those from the large-scale and small-scale tests in this study and those from previous studies on silty soils (Hatami et al. 2010a,b, Khoury et al. 2011).

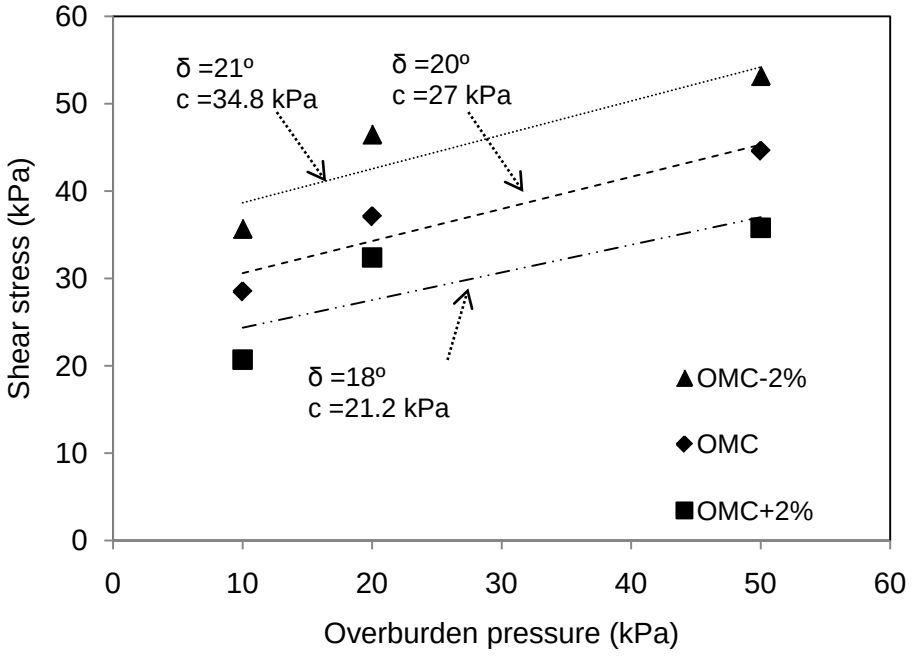


(a)

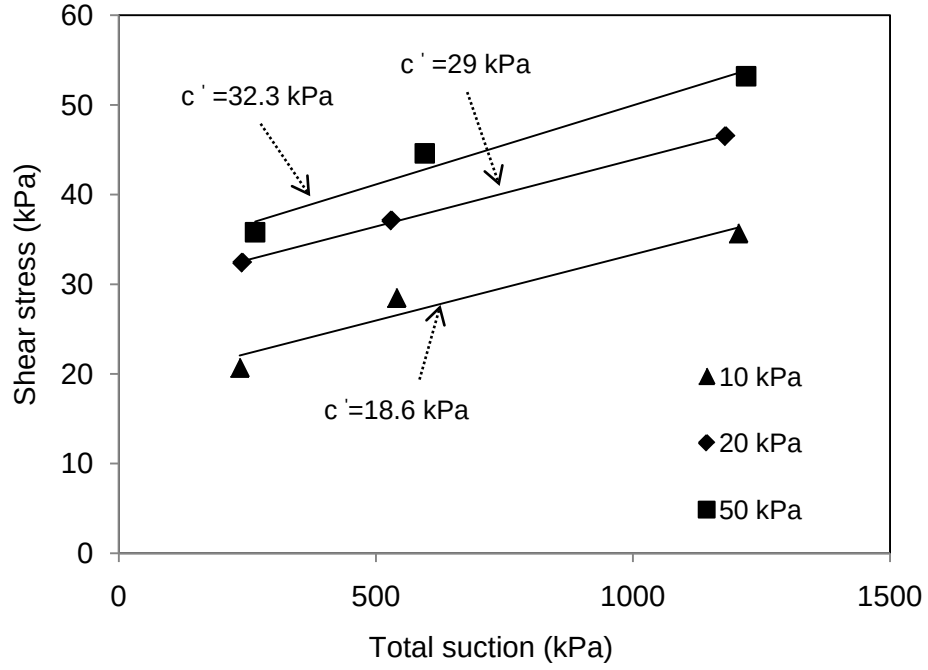


(b)

Figure 35. Mohr-Coulomb envelopes for Chickasha soil-geotextile interface from direct interface shear tests: (a) Envelopes on frontal plane, (b) Envelopes on lateral plane

## 6. MOISTURE REDUCTION FACTOR, $\mu(\omega)$

Based on the results of this study, **Equation 1** is modified in the form:

$$P_r = F^* \alpha \sigma_v' L_e C \mu(\omega) \quad (4)$$

Where $\mu(\omega)$ is the moisture reduction factor and other terms are as defined previously. **Figure 36** shows the variation of $\mu(\omega)$ for the Chickasha soil-Mirafi HP370 geotextile interface as a function of the soil moisture content, with the pullout resistance at ω = OMC-2% taken as the reference value (Hatami et al. 2010a,b).

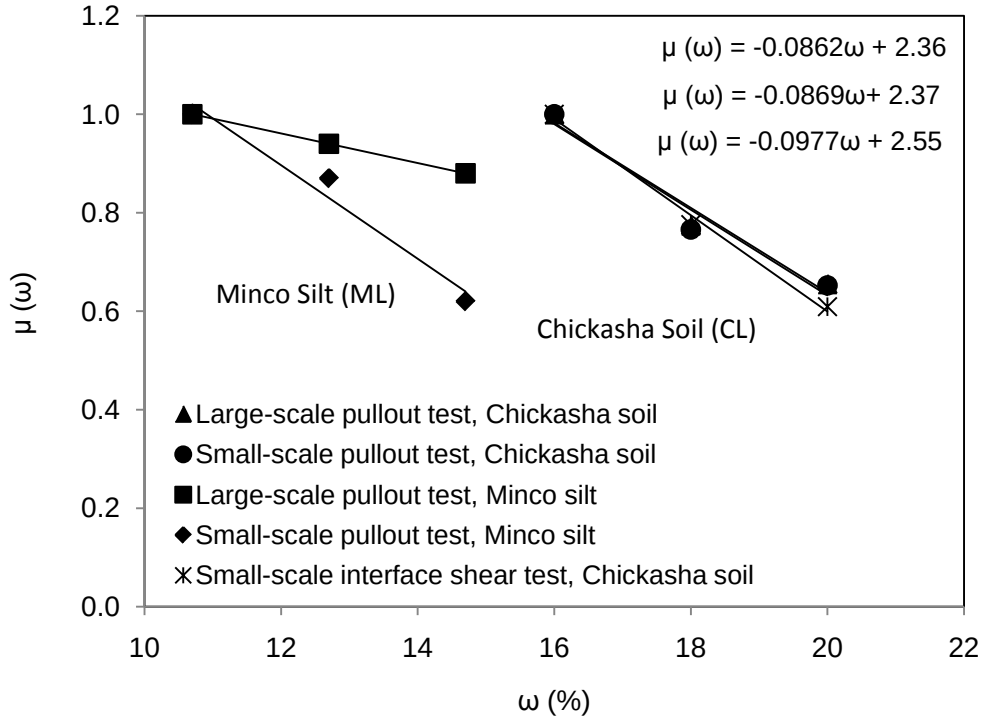


Figure 36. Moisture reduction factor, μ(ω), for the woven geotextile in Chickasha soil from large-scale and small-scale pullout tests (LP, SP and SI indices stand for large-scale pullout, small-scale pullout and small-scale shear interface tests, respectively). The values for Minco silt from a recent study by the authors (Hatami et al. 2010a) are also shown for comparison purposes.

Results shown in **Figure 36** for Chickasha soil indicate that wetting of the soil-geotextile interface during construction or service life of the reinforced soil structure can significantly reduce the pullout resistance of the geotextile reinforcement. The magnitude of the reduction in pullout resistance for the change in the soil moisture content from OMC-2% to OMC+2% in

small-scale and large-scale pullout tests was determined to be approximately 35% and 34%, respectively. The magnitude of this reduction from small-scale shear interface tests was found to be 39%. Results from all tests indicate that $\mu(\omega)$ decreases practically linearly with ω over the range of moisture content values examined in this study. The values for Minco silt from a recent study by the authors are also shown for comparison purposes (Hatami et al. 2010a). Comparison of the results for Chickasha soil with those on Minco silt indicates that the influence of soil moisture content (and hence suction) is more significant in the clay. These results also indicate that the newer tests on the clay yielded more consist results between the large-scale and small-scale tests.

# 7. CONCLUSIONS

The primary objective of this study was to develop a moisture reduction factor [MRF or $\mu(\omega)$] for the pullout resistance of geotextile reinforcement for the design of reinforced soil structures with marginal soils. Based on the results of this study, the current FHWA design equation for pullout resistance of geotextile reinforcement was modified to account for the influence of the marginal soil moisture content on the soil-reinforcement interface strength. The $\mu(\omega)$ values were determined through a series of large-scale and small-scale pullout and interface tests in the laboratory.

Results from both large-scale and small-scale series of tests on Chickasha soil-geotextile interfaces in this study indicated that the change in the soil suction can have a significant influence on the geotextile reinforcement pullout resistance. The test results showed that among the soil moisture conditions examined, the soil compacted at OMC-2% yielded the greatest interface strength properties resulting in the greatest reinforcement pullout resistance. The results also indicate that wetting of the soil-geotextile interface during construction or service life of a reinforced soil structure could reduce adhesion and pullout resistance significantly.

Further testing is in progress to increase the confidence in proposed MRF equations using a different marginal soil that can be used in the reconstruction and stabilization of slopes and retaining structures using the reinforced soil technology.

## 8. REFERENCES


Abu-Farsakh, M., Farrag, K., Almohd, I. and Mohiuddin, A., 2005, "Bearing and Frictional Contributions to the Pullout Capacity of Geogrid Reinforcements in Cohesive Backfill.", *Proceeding of Geo-frontiers, ASCE, Austin, TX*.

Abu-Farsakh M., Coronel J. and Tao M., 2007, " Effect of Soil Moisture Content and Dry Density on Cohesive Soil–Geosynthetic Interactions Using Large Direct Shear Tests.", *Journal of Materials in Civil Engineering, ASCE, Vol. 19, pp. 540-549.*

ASTM International, 2009, "Standard Test Method for Tensile Properties of Geotextiles by the Wide-Width Strip Method.", *American Society for Testing and Materials, West Conshohochen, PA, USA*.

ASTM International, 2010, "Standard Test Method for Measuring Geosynthetic Pullout Resistance in Soil.", *American Society for Testing and Materials, West Conshohochen, PA, USA.*

ASTM International, 2010, "Standard Test Method for Measurement of Soil Potential (Suction) Using Filter Paper.", *American Society for Testing and Materials, West Conshohochen, PA, USA*.

Berg R.B., Christopher, B.R. and Naresh C. Samtani, 2009, "Design and Construction of Mechanically Stabilized Earth Walls and Reinforced Soil Slopes.", *Federal Highway Administration, Washington, DC, USA, FHWA-NHI-10-024.*

Budhu, M., 2000, "Soil Mechanics and Foundations.", *John Wiley & Sons, Inc*.

Campbell, G.S. and W.H. Gardner. 1971, 'Psychometric Measurement of Soil Water Potential: Temperature and Bulk Density Effects.", *Soil Science Society of America Proceedings, Vol.35. pp. 8-11.*

Cardle Fields Company, 2004, *GraphSite v.2.0.1.* http://www.cradlefields.com

Cardoso, R., Romero E., Lima A. and Ferrari A., 2007, "A comparative Study of Soil Suction Measurement Using Two Different High-Range Psychrometers.", *Experimental Unsaturated Soil Mechanics*, *Vol. 112, pp. 79-93.*

Cumbers, J.A. and Nelson, J.D., 2008, "An evaluation of soil suction measurements using the filter paper method and their use in volume change prediction.", *Proceedings of the 1st European Conference on Unsaturated Soils, Durham, UK*.

Elias, V., Christopher, B.R. and Berg, R.R., 2001, "Mechanically Stabilized Earth Walls and Reinforced Soil Slopes-Design and Construction Guidelines.", *Federal Highway Administration, Washington, DC, USA*, *FHWA-NHI-00-043.*

Fredlund, D.G., Morgenstern, N.R., and Widger, R.A., 1978, "The Shear Strength of Unsaturated Soils.", *Canadian Geotechnical Journal, Vol. 15, No. 3, pp. 313-321.*

Fredlund, D.G., Shuai, F., and Freng, M., 2000, "Use of New Thermal Conductivity Sensor for Laboratory Suction.", *Proceedings of the Asian Conference on Unsaturated Soils, Singapore*, *pp. 275-280.*

Hatami, K., Miller G.A., and Garcia L., 2010a, "Use of MSE Technology to Stabilize Highway Embankments and Slopes in Oklahoma.", *Oklahoma Department of Transportation, Tulsa, OK, USA*, *Final Report OTC REOS7-1-19.*

Hatami K., Garcia L.M. and Miller, G.A., 2010b, "Influence of moisture content on the pullout capacity of geotextile reinforcement in marginal soils", *61st Highway Geology Symposium*, *Oklahoma City, OK.*

Hatami K., Garcia L.M. and Miller G.A., 2011, "A Moisture Reduction Factor for Pullout Resistance of Geotextile Reinforcement in Marginal Soils", *Geo-Frontiers, Dallas, TX, ASCE Special Publication No. 211.*

Keller, G.R., 1995, “Experiences with Mechanically Stabilized Structures and Native Soil Backfill.”, *Transportation Research Record*, *1474: 30-38.*

Khoury C.N., Miller G.A. and Hatami K., 2011, “Unsaturated Soil-Geotextile Interface Behavior.”, *Geotextiles and Geomembranes journal, Vol. 29, pp. 17-28.*

McKeen, R. G., 1992, ‘‘A Model for Predicting Expansive Soil Behavior.’’, *Proceedings of the 7th International Conference on Expansive Soils*, *Vol. 1, Dallas, 1–6.*

Miller, G.A. and Hamid, T.B., 2005, “Direct Shear Testing of Interfaces in Unsaturated Soil.”, *Proceedings of EXPERUS, International Symposium on Advances in Experimental Unsaturated Soil Mechanics, Trento, Italy*.

Nam S., Gutierrez M., Diplas P., Petrie J., Wayllace A., Lu N. and Munoz J.J., 2009, “Comparison of Testing techniques and Models for Establishing the SWCC of Riverbank Soils.”, *Engineering Geology Journal*, *Vol. 110, pp. 1-10.*

Ou, F.L., Cox, W. and Collett, L., 1982, “Rock Aggregate Management Planning for Energy Conversation: Optimization methodology.”, *Transportation Research Record*, *872: 63-69.*

Palmeira, E.M., 2004, “Bearing Force Mobilization in Pullout Tests in Geogrids, Geotextiles and Geomembranes.”, *Journal of Geotextiles and Geomembranes, 22: 481-509.*

Pan H., Qing Y. and Pei-yong L., 2010, “Direct and Indirect Measurement of Soil Suction in the Laboratory.”, *Electronic Journal of Geotechnical Engineering, Vol. 15.*

Perera, Y.Y., Padilla, J.M. and Fredlund, D.G., 2004, “Measurement of Soil Suction In Situ using the Fredlund Thermal Conductivity Sensor.”, *Presentation Material for Mining and Waste Management Short Course, Vail, CO*.

Wescor Inc., 2001, HR-33T Dew Point Microvoltmeter Instruction/Service Manual. *Wescor Inc., Lohan, UT*.